

Structural colouration of avian skin: convergent evolution of coherently scattering dermal collagen arrays

Richard O. Prum^{1,*} and Rodolfo Torres²

¹*Department of Ecology and Evolutionary Biology, and Natural History Museum, Dyche Hall, University of Kansas, Lawrence, KS 66045-7561, USA* and ²*Department of Mathematics, University of Kansas, Lawrence, KS 66045-2142, USA*

*Author for correspondence (e-mail: prum@ku.edu)

Accepted 4 April 2003

Summary

Structural colours of avian skin have long been hypothesized to be produced by incoherent (Rayleigh/Tyndall) scattering. We investigated the colour, anatomy, nanostructure and biophysics of structurally coloured skin, ramphotheca and podotheca from 31 species of birds from 17 families in 10 orders from across Aves. Integumentary structural colours of birds include ultraviolet, dark blue, light blue, green and yellow hues. The discrete peaks in reflectance spectra do not conform to the inverse fourth power relationship predicted by Rayleigh scattering. The dermis of structurally coloured skin consists of a thick (100–500 μm) layer of collagen that is usually underlain by a layer of melanin granules. Transmission electron micrographs (TEMs) of this colour-producing dermal collagen layer revealed quasi-ordered arrays of parallel collagen fibres. Two-dimensional (2-D) Fourier analysis of TEMs of the collagen arrays revealed a ring of peak spatial frequencies in the spatial variation in refractive index that are the appropriate size to make the observed ultraviolet–yellow colours by coherent scattering alone. One species, *Philepitta castanea* (Eurylaimidae), has exceptionally ordered, hexagonal arrays of collagen fibres

that produce a hexagonal pattern of spatial frequency peaks in the power spectra. Ultraviolet, blue, green and yellow structural colours of avian skin are produced by coherent scattering (i.e. constructive interference) by arrays of collagen fibres in the dermis. Some yellow and orange skin colours are produced with a combination of structural and pigmentary mechanisms. These combined colours can have reflectance spectra with discrete peaks that are more saturated than hues produced by carotenoid pigments alone. Bluish facial skin from two species of Neotropical antbirds (Thamnophilidae) are nanostructurally too small to produce visible light by coherent scattering, and the colour production mechanism in these species remains unknown. Based on the phylogenetic distribution of structurally coloured skin in Aves, this mechanism of colour production has evolved convergently more than 50 independent times within extant birds.

Key words: structural colour, colour, collagen, integument, nanostructure, Fourier analysis, Aves.

Introduction

The colours of organisms are produced by molecular pigments or by optical interactions with biological nanostructures. The latter structural colours form an important part of the phenotype of many animals (Fox, 1976; Herring, 1994; Parker, 1999) and even some plants (Lee, 1997). Although descriptions of the physical mechanisms of structural colour production are diverse and often redundant (Fox, 1976; Nassau, 1983; Parker, 1999; Srinivasarao, 1999), most mechanisms of structural colour production can be well understood as variations of light scattering at the interfaces of objects that differ in refractive index. (For a fascinating exception in insect cuticle, see Neville, 1975, 1993.)

Accordingly, structural colour production mechanisms can be classified as forms of either incoherent or coherent scattering (van de Hulst, 1981; Bohren and Huffman, 1983).

Incoherent scattering occurs when individual light-scattering objects differentially scatter visible wavelengths (Fig. 1A). Incoherent scattering models require that the light-scattering objects are spatially independent (i.e. randomly distributed with respect to visible wavelengths) so that the phase relationships of the scattered waves are random. Consequently, incoherent scattering models ignore the phase relationships among the scattered waves and describe colour production as the result of differential scattering of wavelengths by the individual scatterers themselves (van de Hulst, 1981; Bohren and Huffman, 1983). By contrast, coherent scattering occurs when the spatial distribution of scatterers is non-random with respect to the wavelengths of visible light, so that the phases of scattered waves are non-random (Bohren and Huffman, 1983). Coherent scattering models describe colour production

in terms of the phase interactions among light waves scattered by multiple scatterers (Fig. 1B). Scattered waves that are out of phase destructively interfere and cancel one another, whereas scattered waves that are in phase will constructively

reinforce one another and are coherently reflected. In incoherent scattering, colour is a function of the properties of individual scatterers, whereas in coherent scattering colour is determined by the spatial distribution of light-scattering interfaces (Fig. 1).

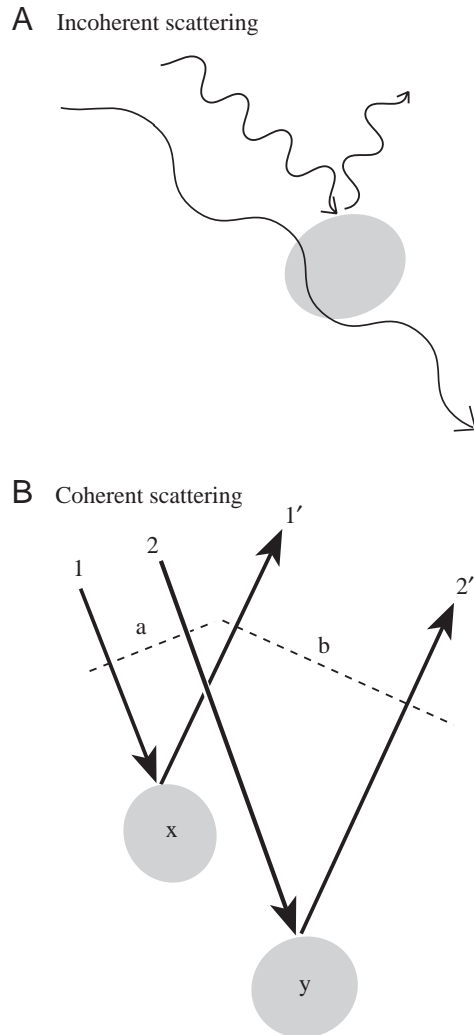


Fig. 1. Comparison of incoherent and coherent scattering mechanisms of biological structural colour production. (A) Incoherent scattering is differential scattering of wavelengths by individual light-scattering objects. In Rayleigh (also known as Tyndall) scattering, smaller wavelengths are preferentially scattered. The phase relationships among light waves scattered from different objects are ignored and assumed to be random. (B) Coherent scattering is differential interference or reinforcement of wavelengths scattered by multiple light-scattering objects (x , y). Coherent scattering of specific wavelengths is determined by the phase relationships among the scattered waves. Scattered wavelengths that are out of phase will cancel each other out, but scattered wavelengths that are in phase will be constructively reinforced and coherently scattered. Phase relationships of wavelengths scattered by two different objects (x , y) are given by the differences in the path lengths of light scattered by the first object (x : $1-1'$) and a second object (y : $2-2'$) as measured from planes perpendicular to the incident (a) and reflected (b) waves in the mean refractive index of the media.

Incoherent scattering models include Rayleigh scattering (also erroneously known as Tyndall scattering; see Young, 1982) and Mie scattering, which is a mathematically exact description of light scattering by single particles that simplifies to the Rayleigh scattering for small particle sizes (van de Hulst, 1981; Bohren and Huffman, 1983). Examples of incoherent scattering include blue sky, blue smoke, blue ice and blue snow. Coherent scattering encompasses various optical phenomena that can also be described as diffraction, reinforcement and interference. Well-known examples include the structural colours produced by brilliant iridescent butterfly wing scales and avian feather barbules such as the peacock's tail (Fox, 1976; Ghiradella, 1991; Parker, 1999).

Coherent scattering often produces the phenomenon of iridescence – a prominent change in hue with angle of observation or illumination. Iridescence occurs if changes in the angle of observation or illumination affect the mean path length of scattered waves; such a change will affect the phase relationships among the scattered waves and change which wavelengths are constructively reinforced after scattering. Iridescence conditions are met when the light-scattering objects are arranged in laminar or crystal-like arrays. By contrast, incoherent scattering does not yield iridescence. In the biological literature, at least since Mason (1923), iridescence has been often synonymized with coherent scattering (e.g. Fox, 1976; Nassau, 1983; Lee, 1991, 1997; Herring, 1994). Consequently, all iridescent structural colours were hypothesized correctly to be due to coherent scattering, but all non-iridescent structural colours were erroneously hypothesized to be exclusively due to incoherent scattering (e.g. Fox, 1976; Herring, 1994).

Recently, however, it has been demonstrated that coherent light scattering by quasi-ordered arrays of light scatterers can produce biological structural colours that are not strongly iridescent (Prum et al., 1998, 1999a,b). Quasi-ordered arrays have unimodal distributions of size and spacing but lack laminar or crystal-like organization at larger spatial scales that produce iridescence. Quasi-ordered arrays have a similar organization to a bowl of popcorn; each popped kernel is similar in size to its neighbour, and centre-to-centre distances are quite similar, but beyond the spatial scale of a single kernel there is no organization. An example of a colour-producing nanostructure is the light-scattering air bubbles in the medullary keratin of structurally coloured avian feather barbules; these air-keratin matrices are sufficiently spatially ordered at the nanoscale level to produce the observed hues by coherent scattering but are not ordered at larger spatial scales (Prum et al., 1998, 1999b), so these colours are not iridescent or are only weakly iridescent (Osorio and Ham, 2002).

In order to describe the spatial periodicity and to analyze the optical properties of quasi-ordered biological arrays, we have

developed an application of the two-dimensional (2-D) Fourier transform to structural colour production (Prum et al., 1998, 1999a,b). Based on transmission electron micrographs (TEMs) of the tissues, the method permits the characterization of the spatial periodicity of the tissue in multiple directions and the prediction of the hue, and potentially iridescence, of its colour. This method is designed to test whether light scatterers are spatially independent – a fundamental assumption of incoherent scattering models – and whether the biological arrays are appropriately nanostructured to produce the observed colours by coherent scattering.

Structural colours of avian skin

Non-iridescent structural colours occur in the skin, bill (ramphotheca), legs and feet (podotheca) of a broad diversity of birds from many avian orders and families (Figs 2, 3). Auber (1957) reported structurally coloured skin in 19 avian families from 11 avian orders (Table 1). Auber (1957) assumed that all blue or green skin colours are structural rather than pigmentary because blue and green pigments are unknown or very rare, respectively, in the avian integument (Fox, 1976). Using the same conservative criterion, we have identified structurally coloured skin, ramphotheca and podotheca in 129 avian genera in 50 families from 16 avian orders (Table 1). Structurally coloured skin is apparently present in more than 250 bird species, or roughly more than 2.5% of avian biological species.

Because they are noniridescent, structural colours of avian skin were long hypothesized traditionally to be produced by Rayleigh (or Tyndall) scattering (Camichel and Mandoul, 1901; Mandoul, 1903; Tièche, 1906; Auber, 1957; Rawles, 1960; Lucas and Stettenheim, 1972; Fox, 1976). The light-scattering structures were variously hypothesized to be melanin granules, biological colloids or turbid media of proteins, lipids, etc. in the dermis. The Rayleigh scattering hypothesis was never actually tested with either spectrophotometry – to examine whether these structural colours conform to the prediction of Rayleigh's inverse fourth power law – or with electron microscopy – to examine whether



Fig. 2. Structurally coloured ornaments of a sample of the non-passeriform birds examined: (A) *Dromaius novaehollandiae*, (B) *Oxyura jamaicensis*, (C) *Numida meleagris*, (D) *Lophura bulweri*, (E) *Tragopan temminckii*, (F) *Tragopan caboti*, (G) *Syrigma sibalatrix*, (H) *Ptilerodius pileatus* and (I) *Opisthocomus hoazin*. A, reproduced with permission from Nate Rice; B,D–F, reproduced with permission from Kenneth Fink; C,H,I, reproduced with permission from VIREO; G, reproduced with permission from Roger Boyd.

the hypothesized light-scattering objects were spatially independent. Green integumentary colours were further hypothesized to be a combination of Rayleigh-scattering blue and carotenoid yellow (e.g. Fox 1976) but this was never confirmed.

Prum et al. (1994) were the first to examine structurally coloured avian skin with electron microscopy. We documented that the green and blue colours of the supraorbital caruncles of the male velvet asity *Philepitta castanea* (Eurylaimidae) of Madagascar are produced by coherent scattering from hexagonally organized arrays of parallel collagen fibres in the dermis. Subsequently, Prum et al. (1999a) performed a comparative analysis of the anatomy, nanostructure and structural colouration of three species of the Malagasy asities. We applied the 2-D Fourier method to asity caruncle collagen arrays to confirm the coherent scattering mechanism and to describe the variations in hue produced by variations in

collagen nanostructure. We also documented that the crystal-like hexagonal nanostructure of *Philepitta* is derived from the plesiomorphic, quasi-ordered nanostructure of the sunbird asities *Neodrepanis*. Elsewhere in animals, colour-producing, quasi-ordered collagen arrays have only been described in the tapetum lucidum of the sheep eye (Bellairs et al., 1975).

With the exception of the asities (Eurylaimidae; Prum et al.,

1994, 1999a), the incoherent scattering hypothesis of structural colour production in avian skin has not been tested. Here, we used fibre-optic spectrophotometry, light microscope histology, TEM and 2-D Fourier analysis of TEM images to investigate structurally coloured skin, ramphotheca and podotheca from 31 species of birds from 17 families in 10 different orders (Table 2).

The sample includes an ecologically diverse collection of birds with a wide variety of colours from across avian phylogeny, from the paleognathes to the passerines (Figs 2, 3).

Materials and methods

Species sampled and microscopy

Structurally coloured tissue specimens were obtained from salvaged, frozen or recently collected specimens from a broad variety of species (Table 2) from zoos, private collections and scientific collecting in North America, South America, Africa and Madagascar. Most specimens were fixed in 2.5% glutaraldehyde for 1–4 h and were then transferred to and stored in 0.1 mol l⁻¹ cacodylate buffer (0.1 mol l⁻¹ sodium cacodylate, 2.5 mmol l⁻¹ calcium chloride, 4% sucrose). Some specimens were originally fixed in 10% formalin and then refixed in 2.5% glutaraldehyde before microscopy. At the time of death or thawing (for salvaged birds), the colour of the skin was observed and recorded visually, and often a photograph was taken.

For light microscopy, specimens of structurally coloured skin from nine species were embedded in paraffin, cut into 10 µm sections and stained with Masson's trichrome, which includes the collagen-specific stain Fast Green. For TEM, skin and ramphotheca samples were placed in Karnovsky fixative (2.5% glutaraldehyde, 2.5% paraformaldehyde) for 2 h at 4°C. They were then post-fixed in 2–4% osmium tetroxide for 1.5 h. They were then stained with 2% aqueous uranyl acetate for 1 h. Tissue pieces were then



Fig. 3. Structurally coloured ornaments of a sample of the piciform and passeriform birds examined: (A) *Selenidera reinwardtii*, (B) *Ramphastos vitellinus*, (C) *Ramphastos toco*, (D) *Neodrepanis coruscans*, (E) *Philepitta castanea*, (F) *Myrmeciza ferruginea*, (G) *Gymnophis leucapsis*, (H) *Procnias alba*, (I) *Perissocephalus tricolor*, (J) *Dyaphorophya concreta*, (K) *Tersiphone mutata* and (L) *Leucopsar rothschildi*. A,F–J, reproduced with permission from VIREO; B,C,L, reproduced with permission from Kenneth Fink; H, reproduced with permission from Nate Rice; D, reproduced with permission from Steve Zack; K, reproduced with permission from Tom Schulenberg.

Table 1. Provisional list of avian families with structurally coloured violet, blue or green skin, ramphotheca or podotheca

Order	Family	Species
Casuariiformes	Casuariidae*	<i>Dromaius</i> , <i>Casuarius</i>
Anseriformes	Anatidae*	<i>Anas</i> , <i>Oxyura</i> †, <i>Aythya</i> , <i>Dendrocygna</i>
Galliformes	Megapodidae	<i>Aepyodius arfakianus</i> , <i>Alectrura lathamii purpureicollis</i>
	Cracidae*	<i>Chaemaphetes</i> , <i>Aburria</i> , <i>Penelope</i> , <i>Pauxi</i> , <i>Crax</i>
	Numididae*	<i>Numida</i> , <i>Guttera</i>
	Phasianidae*	<i>Tragopan</i> †, <i>Lophura</i> †, <i>Lophophorus</i> , <i>Ithaginis</i> , <i>Argusianus</i> , <i>Pavo</i> , <i>Gallus</i> , <i>Meleagris</i> , <i>Agriocharis</i>
Pelicaniformes	Sulidae	<i>Sula</i>
	Pelecanidae	<i>Pelecanus conspicillatus</i>
	Phalacrocoracidae	<i>Phalacrocorax</i>
	Anhigidae	<i>Anhinga anhinga</i>
Ciconiiformes	Ardeidae*	<i>Syrigma</i> , <i>Pilherodius</i> , <i>Egretta</i> , <i>Casmerodius</i> , <i>Ardeola</i> , <i>Nycticorax</i> , <i>Ixobrychus</i>
	Ciconiidae	<i>Ciconia abdimii</i>
	Threskiornithidae	<i>Bostrichya</i> , <i>Pseudibis</i> , <i>Ajaia</i>
Falconiformes	Accipitridae	<i>Aegyptius</i> , <i>Trigonoceps</i> , <i>Torgos</i>
	Falconidae	<i>Falco berigora</i>
Gruiformes	Cariamidae	<i>Cariama</i>
	Rallidae	<i>Porphyrio martinica</i> , <i>Porphyryula alleni</i> , <i>Gymnocrex</i>
	Heliornithidae	<i>Heliopais personata</i>
Charadriiformes	Jacaniidae	<i>Jacana</i> , <i>Actophilornis</i> , <i>Metopidius</i>
	Recurvirostridae	<i>Recurvirostra</i>
	Sternidae	<i>Gygis</i>
Psittaciformes	Psittacidae	<i>Cacatua</i>
Columbiformes	Columbidae	<i>Macropygia</i> , <i>Zenaida</i> , <i>Lopholaimus</i> , <i>Ducula bicolor</i> , <i>Treron</i>
Opisthocomiformes	Opisthocomidae*	<i>Opisthocomus hoazin</i>
Cuculiformes	Cuculidae*	<i>Coua</i> , <i>Morococcyx</i> , <i>Geococcyx</i> , <i>Neomorphus</i> , <i>Ceuthmochares</i> , <i>Phoenicophaeus</i> , <i>Carpococcyx</i>
Trogoniformes	Trogonidae	<i>Apaloderma</i> , <i>Harpactes</i> , <i>Trogon melanocephalus</i>
Coraciiformes	Bucerotidae	<i>Bucorvus</i> , <i>Tockus</i> , <i>Bucerotus</i> , <i>Ceratogymna</i> , <i>Aceros</i> , <i>Anorhinus</i> , <i>Berenicornis</i> , <i>Rhyticeros</i>
	Picidae	<i>Blythipicus</i> , <i>Picus</i>
Passeriformes	Ramphastidae*	<i>Selenidera</i> , <i>Ramphastos</i> , <i>Pteroglossus</i>
	Eurylaimidae*	<i>Eurylaimus</i> , <i>Cymbirhynchus</i> , <i>Neodrepanis</i> †, <i>Philepitta</i> †
	Thamnophilidae*	<i>Gymnopathys</i> , <i>Myrmeciza</i> , <i>Rhegmatorhina</i> , <i>Phaenostictus</i> , <i>Gymnocichla</i> , <i>Myrmoderus</i>
	Formacariidae	<i>Formacarius</i>
	Cotingidae*	<i>Perissocephalus tricolor</i> , <i>Procnias nudicollis</i> †, <i>Gymnoderus foetidus</i>
	Sturnidae*	<i>Leucopsar rothschildi</i>
	Timaliidae	<i>Garrulax</i> , <i>Stachyris erythroptera</i>
	Pycnonotidae	<i>Bleda syndactyla</i> , <i>Criniger calurus</i>
	Platysteridae	<i>Dyaphorophygia</i> (= <i>Platysteira</i>)
	Monarchidae*	<i>Terpsiphone</i> , <i>Arses</i> , <i>Hypothymis</i> , <i>Pseudobias</i>
	Picathartidae	<i>Picathartes oreas</i>
	Paradisaeidae	<i>Paradigalla</i> †, <i>Cicinnurus</i> †, <i>Epimachus</i> †
	Cnemophilidae	<i>Loboparadisea</i> †
	Troglodytidae	<i>Cyphorhynchus phaeocephalus</i>
	Meliphagidae	<i>Melidectes</i> , <i>Philemon</i> , <i>Entomyzon</i> , <i>Melithreptus</i> , <i>Lichenostomus cratitius</i> , <i>Certhionyx</i>
	Orthonychidae	<i>Orthonyx spaldingii</i>
	Callaeidae	<i>Callaeas cinerea</i>
	Oriolidae	<i>Sphecotheres viridis</i>
	Vangidae	<i>Leptopterus</i> , <i>Cyanolaimus</i> , <i>Euryceros</i> , <i>Schetba</i>
Prionopidae	<i>Prionops scopifrons</i>	
Icteridae	<i>Psarocolius</i> , <i>Gymnomystax</i> , <i>Icterus icterus</i>	
Estrildidae	<i>Pyrenestes</i> , <i>Hypargos</i>	

Families marked with an asterisk are listed by Auber (1957).

†Indicates strong sexual dimorphism in structural colouration.

Table 2. *Features of structurally coloured skin specimens examined*

Taxon	Observed colour	Observed peak reflectance λ_{\max} (nm)	Peak spatial frequency (nm^{-1})	Fourier-predicted colour	Fourier-predicted peak reflectance λ_{\max} (nm)	<i>N</i>
Casuariiformes						
Casuariidae (cassowaries)						
<i>Dromaius novaehollandiae</i>	Light blue	–	0.0065	Light blue	470	3
Anseriformes						
Anatidae (ducks)						
<i>Oxyura jamaicensis</i>	Light blue	465	0.0053	Yellow	580	4
Galliformes						
Cracidae (guans)						
<i>Chaemaphetes unicolor</i>	Dark blue	–	0.0076	Dark blue	370	3
Numididae (guineafowl)						
<i>Numida meleagris</i>	Light blue	–	0.0063	Light blue	440	7
Phasianidae (pheasants)						
<i>Tragopan temmincki</i>						
	Dark blue	352	0.0068	Dark blue	340	17
	Light blue	465	0.0065	Light blue	480	8
<i>Tragopan caboti</i>						
	Dark blue	449	0.0078	Dark blue	350	12
	Light blue	450	0.0067	Dark blue	390	7
	Orange	603	0.0051	Yellow	580	8
<i>Tragopan satyra</i>						
	Dark blue	366	0.0073	Dark blue	350	16
<i>Lophura bulweri</i>						
	Deep blue	340	0.0071	Dark blue	400	19
<i>Lophophorus impejanus</i>						
	Deep blue	350	0.0071	Dark blue	400	7
<i>Meleagris gallipavo</i>						
	Blue	–	0.0097	Dark blue	330	3
Pelecaniformes						
Sulidae (gannets and boobies)						
<i>Sula nebouxii</i>	Light blue	–	0.0065	Dark blue	410	14
Ciconiiformes						
Ardeidae (herons)						
<i>Pilherodius pileatus</i>	Light blue	579	0.0065	Light blue	480	11
<i>Syrigma sibilatrix</i>	Light blue	533	0.0059	Light blue	470	26
Opisthocomiformes						
Opisthocomidae (hoatzin)						
<i>Opisthocomus hoazin</i>	Blue	–	0.0083	Ultraviolet	300	4
Cuculiformes						
Cuculidae (cuckoos)						
<i>Coua caerulea</i>	Dark blue	399	0.0077	UV–blue	360	3
<i>Coua reynaudii</i>	Dark blue	–	0.0075	Dark blue	400	7
<i>Ceuthmochares aereus</i>	Yellow	–	0.0055	Green	530	13
Trogoniformes						
Trogonidae (trogons)						
<i>Apaloderma aequatoriale</i>	Yellow	530	0.0043	Yellow	600	3
Piciformes						
Ramphastidae (barbets and toucans)						
<i>Selenidera culik</i>	Turquoise	487	0.0057	Turquoise	490	6
<i>Ramphastos vitellinus</i>						
	Facial skin	Blue	0.0055	Blue	440	4
	Ramphotheca	Blue	0.0053	Green	520	5
<i>Ramphastos toco</i>						
	UV–blue	360	0.0057	Dark blue	400	10
	Yellow	550–750	0.0036	Red	720	5

Table 2. Continued

Taxon	Observed colour	Observed peak reflectance λ_{\max} (nm)	Peak spatial frequency (nm^{-1})	Fourier-predicted colour	Fourier-predicted peak reflectance λ_{\max} (nm)	<i>N</i>
Passeriformes						
Eurylaimidae (broadbills and asities)						
<i>Neodrepanis coruscans</i>	Dark blue	417	0.0082	Ultraviolet	349	
	Blue	517	0.0072	Dark blue	400	
<i>Neodrepanis hypoxantha</i>	Dark blue	403	0.0083	Ultraviolet	360	
	Light blue	465	0.0065	Blue	440	
<i>Philepitta castanea</i>	Light blue	483	0.0064	Dark blue	387	
	Green	528	0.0064	Dark blue	410	
Thamnophilidae (antbirds)						
<i>Gymnophrys leucapsis</i>	Light blue	–	0.0105	–	–	4
<i>Rhegmatorhina melanosticta</i>	Light blue	–	0.0136	–	–	4
<i>Myrmeciza ferruginea</i>	Light blue	–	0.0053	Light blue	480	4
Cotingidae (cotingas)						
<i>Perissocephalus tricolor</i>	Dark blue	–	0.0068	Light blue	470	5
<i>Procnias nudicollis</i>	Green	–	0.0053	Green	510	5
Platysteridae (wattle-eyes)						
<i>Dyaphorophya concreta</i>	Yellow-green	535	0.0061	Turquoise	490	10
Monarchidae (monarch flycatchers)						
<i>Terpsiphone mutata</i>	Dark blue	–	0.0083	Dark blue	330	3
Sturnidae (starlings)						
<i>Leucopsar rothschildi</i>	Dark blue	–	0.0070	Dark blue	430	4
Data reported for the three species of Eurylaimidae are from Prum et al. (1999a). <i>N</i> represents transmission electron microscopy (TEM) image sample size.						

dehydrated through an ethanol series and embedded in Eponate 12. They were sectioned with a diamond knife to a thickness of approximately 100 nm. Specimens were viewed with a transmission electron microscope (JEOL 12000 EXII; Peabody, MA, USA). TEM micrographs were taken with Polaroid negative film or were digitally captured using a Soft-Imaging Megaview II CCD camera (1024 pixels×1200 pixels). Numerical analysis was conducted directly on the digital images or on the photograph negatives after scanning at a resolution of 300 d.p.i.

Spectrophotometry

If a substantial component of the original structural colour was preserved after freezing or fixation, the reflectance spectra of the structurally coloured tissues were measured using an S2000 fibre optic diode-array spectrometer with a PX-2 pulsed xenon light source (Ocean Optics, Dunedin, FL, USA). This spectrometer produces 2048 reflectance data points between 160 nm and 865 nm (or 1520 data points in the range of 300–800 nm) with a mean error of 0.14 nm. Measurements were made with perpendicularly incident light from approximately 2–3 mm away from the specimen for an illuminated field of approximately 3 mm² with 100 ms summation time. A Spectralon diffuse reference standard from Ocean Optics was used as a white standard, and the ambient

light of a darkened room was used as a dark reference. Percent reflectance (%*R*) was calculated by:

$$\%R = [(S - D)/(W - D)] \times 100, \quad (1)$$

where *S* is the reflectance of the specimen, *D* is the reflectance of a dark standard, and *W* is the reflectance of a white standard.

2-D Fourier analysis

Coherent scattering of visible wavelengths is a consequence of nanoscale spatial periodicity in refractive index of a tissue. Following a theory of corneal transparency by Benedek (1971), Prum et al. (1998, 1999a,b) developed an application of the discrete Fourier 2-D transform to analyze the periodicity and optical properties of structural coloured tissue. Discrete Fourier analysis transforms a sample of data points into an equivalent sum of component sine waves of different frequencies and amplitudes (Briggs and Henson, 1995). The amplitudes of each Fourier component wave express the relative contribution of that frequency of variation to the periodicity of the original data. The variation in the squared amplitudes over all Fourier components is called the Fourier power spectrum. The relative values of the different Fourier components in the power spectrum express the comparative contribution of those frequencies of variation to the original function. This application of Fourier analysis is derived independently from

electromagnetic optical theory (Benedek, 1971) and is distinct from the traditional physical field of 'Fourier optics', although they both describe coherence among scattered light waves.

The digital or digitized TEM images were analyzed using the matrix algebra program MATLAB (Version 5.2; MATLAB, 1992) on a Macintosh computer. The scale of each image (nm pixel^{-1}) was calculated from the number of pixels in the scale bar of the micrograph. The largest available square portion of the array was then selected for analysis; for most images, this area was 1024 pixels^2 , but for a few images was as small as 600 pixels^2 . The mean refractive index of each tissue was estimated by generating a two-partition histogram of image darkness (i.e. the distribution of darker and lighter pixels). The frequency distribution of darker and lighter pixels was used to estimate the relative frequency of collagen and mucopolysaccharide in the image and to calculate a weighted mean refractive index for the tissue. Previously, we have used estimates of the refractive indices of collagen and the mucopolysaccharide matrix between collagen fibres of 1.51 and 1.35, respectively (Prum et al., 1994, 1999a), taken from Maurice (1984). Recently, however, more-refined methods have estimated the refractive indices of collagen and mucopolysaccharide as 1.42 and 1.35, respectively (Leonard and Meek, 1997).

The numerical computation of the Fourier transform was done with the well-established 2-D fast Fourier transform (FFT2) algorithm (Briggs and Henson, 1995). We calculated the 2-D Fourier power spectrum, or the distribution of the squares of the Fourier coefficients. The 2-D Fourier power spectrum resolves the spatial variation in refractive index in the tissue into its periodic components in any direction from a given point. The 2-D Fourier power spectra are expressed in spatial frequency (nm^{-1}) by dividing the initial spatial frequency values by the length of the matrix (pixels in the matrix $\times \text{nm pixel}^{-1}$). Each value in the 2-D power spectrum reports the magnitude of the periodicity in the original data of a specific spatial frequency in a given direction from all points in the original image. The spatial frequency and direction of any component in the power spectrum are given by the length and direction, respectively, of a vector from the origin to that point. The magnitude is depicted by the colour (from blue to red), but the units are dimensionless values related to the total darkness of the original digital images.

We calculated radial means of the power spectra using 100 spatial frequency bins, or annuli, between 0 nm^{-1} and 0.02 nm^{-1} and expressed them in % total Fourier power. Composite radial means were calculated from a sample of power spectra from multiple TEM images to provide an indication of the predominant spatial frequency of variation in refractive index in the tissue over all directions.

We also produced predicted reflectance spectra based on the 2-D Fourier power spectra, image scales and mean refractive indices. First, a radial mean of the % power was calculated for concentric bins, or annuli, of the power spectrum corresponding to 50 10 nm-wide wavelength intervals between 300 nm and 800 nm (covering the entire avian visible

spectrum). The radial mean power values were expressed in % visible Fourier power by normalizing the total power values across all potentially visible spatial frequencies (i.e. potentially scattering light between 300 nm and 800 nm) to 1. The inverse of the spatial frequency means for each wavelength were then multiplied by twice the mean refractive index of the medium and expressed in terms of wavelength (nm). A few images depict oblique, elliptical sections of the cylindrical collagen fibres, which will bias the predicted hue towards longer wavelengths. In these cases, the radial mean was calculated from a single quadrant or from a custom radial section of the power spectrum. A composite predicted reflectance spectra for each tissue was produced by averaging the normalized predicted spectra from a sample of TEM images. The result is a theoretical prediction of the relative magnitude of coherent light scattering by the tissue that is based entirely on the spatial variation in refractive index of the tissue.

Results

Colour and spectrophotometry

The structural colours of the 31 species observed varied widely in hue from ultraviolet, dark blue, blue, light blue, turquoise, green and yellow (Fig. 4; Table 2). In addition, yellow and orange hues that are produced by a combination of structural and pigmentary mechanisms (see below) were observed. Peak wavelength (λ_{max}) varied among the species measured from 340 nm in *Lophura bulweri* (Phasianidae), a brilliant ultraviolet hue (Figs 2D, 4B), to 535 nm in *Dyaphorophya concreta* (Platysteiridae), a yellowish green (Figs 3J, 4I). Although the preserved specimen did not have a measurable reflectance spectra, the purely structural colour of facial skin of *Ceuthmochares aereus* (Cuculidae) is a brilliant yellow. Many species had substantial or predominant ultraviolet components in their structural colours, which are visible to birds but not to humans (Burkhardt, 1989; Jacobs, 1992; Derim-Oglu, 1994; Hart, 2001). Several species had complex variation in hue within a single skin patch or ornament. For example, *Tragopan temminckii* displays vivid structural ultraviolet, dark blue, light blue and turquoise, along with pigmentary blood red in adjacent sections of its throat lappet (Fig. 2E). The central field of the *T. temminckii* lappet features an array of light blue spots on a vividly ultraviolet background. Although the light blue spots appear to be much more brilliant to human vision (Fig. 2E), the dark blue background colour is equivalently brilliant in the ultraviolet wavelengths that are not visible to humans (Fig. 4D,E).

None of the reflectance spectra from the 14 species measured showed the inverse fourth power relationship predicted by Rayleigh scattering. Each reflectance spectrum revealed a discrete peak or a pair of peaks. The lower-wavelength (i.e. left-hand) slopes of the spectra are not caused by absorption (e.g. Finger, 1995), because the peaks are at substantially longer wavelengths than the beginning of the absorption spectrum of collagen (approximately 290 nm).

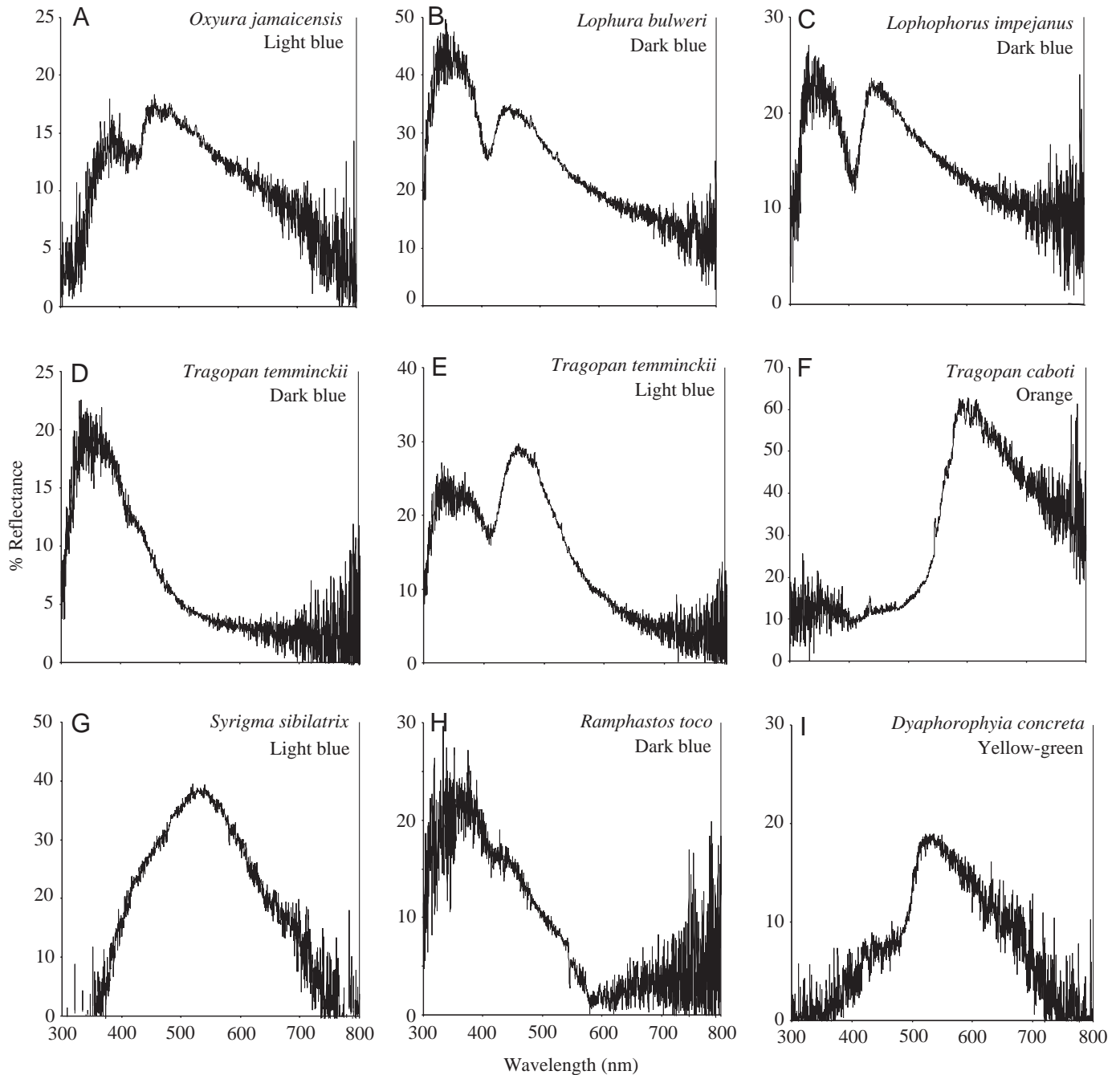


Fig. 4. Reflectance spectra of structurally coloured avian ornaments: (A) *Oxyura jamaicensis*, light blue; (B) *Lophura bulweri*, dark blue; (C) *Lophophorus impejanus*, dark blue; (D) *Tragopan temminckii*, dark blue; (E) *Tragopan temminckii*, light blue; (F) *Tragopan caboti*, orange; (G) *Syrigma sibilatrix*, light blue; (H) *Ramphastos toco*, dark blue and (I) *Dyaphorophya concreta*, yellow-green.

However, reflectance spectra from a number of diverse galliform species exhibit dual peaks: one in the ultraviolet (approximately 350 nm) and another in the blue portion of the spectrum (approximately 410 nm) (Fig. 4A-C,E). The highly repeated position of the dip in multiple reflectance spectra between the two peaks at approximately 400 nm may indicate selective absorption of these wavelengths by some unknown pigment or component of the epidermis. These features of the reflectance spectra were not adequately explained by Fourier-

predicted reflectance spectra (see below) and currently require some additional explanation.

None of these structural colours was iridescent, although under a dissection microscope, local (approximately 500 μm scale) variations in colour could be observed among different areas of the skin. In many samples, the hue could be changed or eliminated (i.e. turned white) by compression on the surface of the skin with forceps. Presumably, this occurs because of deformation of the colour-producing dermal collagen arrays.

Anatomy

Structurally coloured skin samples of nine species were examined with light microscope histology (Fig. 5). Most species had a thin epidermis between 12 μm and 50 μm thick. Below the epidermis was a substantial colour-producing, dermal collagen layer that varied, in most cases, between 200 μm and 500 μm in thickness (Figs 5, 6A–C). In most species, this collagen layer was underlain by a thick and continuous layer of melanin granules parallel to the surface of the skin that completely covered the deeper dermal tissue (Figs 5, 6C). One species, *Procnias nudicollis* (Cotingidae), had a substantially thicker collagen layer of 500–1000 μm with little or no melanin in the underlying dermis (Fig. 5H). Even without histological examination, it was easily observed that two species of Neotropical antbirds, *Gymnopithys leucapsis* and *Rhegmatorhina melanosticta* (Thamnophilidae), clearly lack any melanin deposition in the skin (also confirmed by TEM) (not shown).

The morphology of structurally coloured bird skin was quite distinct from that of uncoloured white skin and from that of bright red skin in the same or closely related species. For example, unpigmented white leg skin from *P. nudicollis* was less than 75 μm thick (Fig. 5G), or an order of magnitude thinner than the structurally coloured avian skin of *P. nudicollis* and other bird species. In the red lateral patches of the throat lappet of *T. temminckii* (Fig. 2E), *Tragopan satyra* and *Tragopan caboti* (Fig. 2F) and the red facial skin of the toucan *Bailloni bailloni* (Ramphastidae; not illustrated), the dermis showed abundant capillaries immediately below the epidermis and greatly reduced or no underlying melanin deposition (Fig. 5I). Purely structurally coloured bird skin also differs from carotenoid pigmented skin. In *Ramphastos toco* (Fig. 3C), the yellow facial skin has abundant carotenoid-containing lipid vacuoles within the epidermis and a complete lack of melanin deposition (Fig. 6F). The adjacent, structurally coloured, ultraviolet eye ring completely lacks epidermal lipid

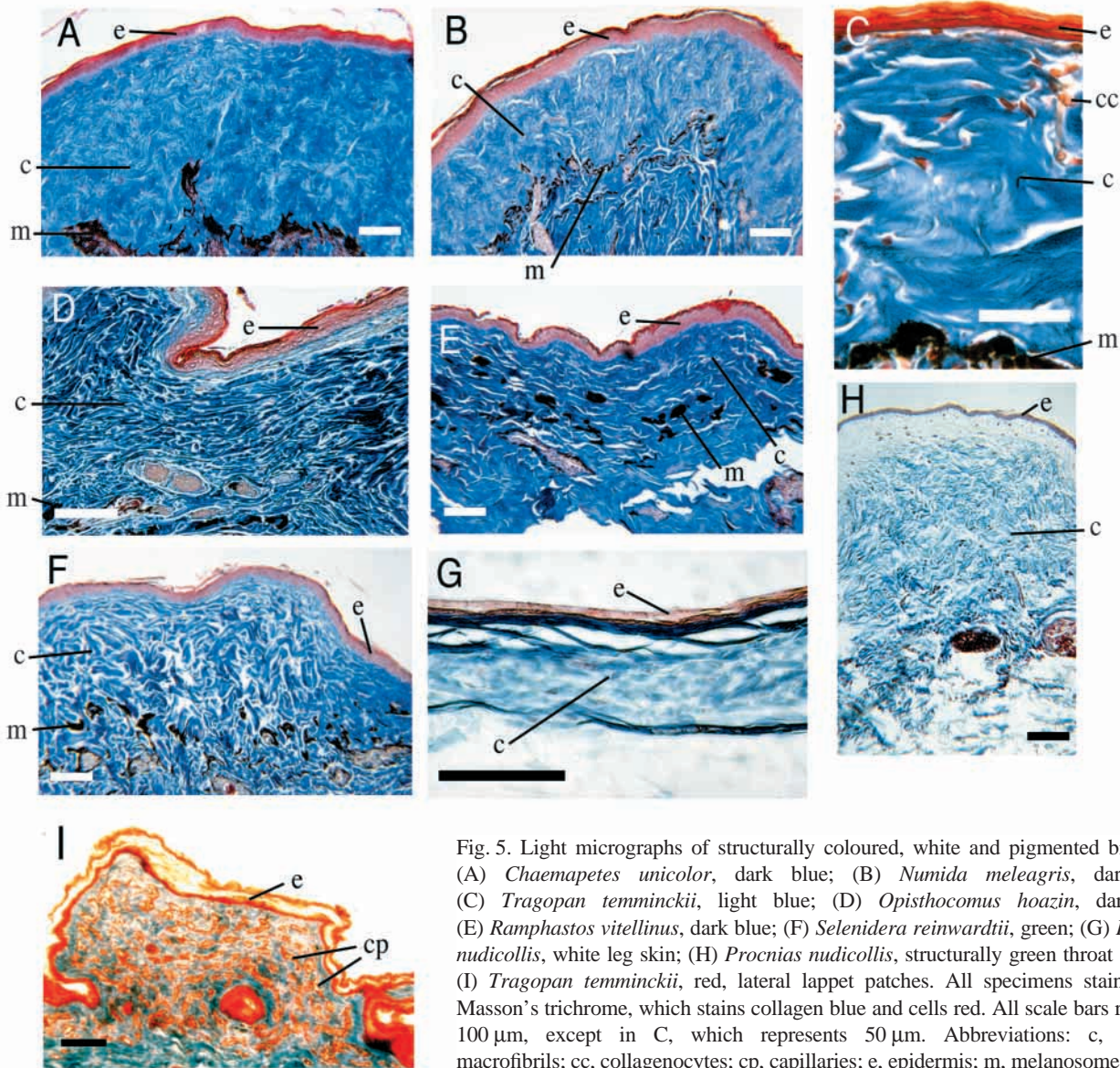


Fig. 5. Light micrographs of structurally coloured, white and pigmented bird skin: (A) *Chaemapetes unicolor*, dark blue; (B) *Numida meleagris*, dark blue; (C) *Tragopan temminckii*, light blue; (D) *Opisthocomus hoazin*, dark blue; (E) *Ramphastos vitellinus*, dark blue; (F) *Selenidera reinwardtii*, green; (G) *Procnias nudicollis*, white leg skin; (H) *Procnias nudicollis*, structurally green throat skin and (I) *Tragopan temminckii*, red, lateral lappet patches. All specimens stained with Masson's trichrome, which stains collagen blue and cells red. All scale bars represent 100 μm , except in C, which represents 50 μm . Abbreviations: c, collagen macrofibrils; cc, collagenocytes; cp, capillaries; e, epidermis; m, melanosomes.

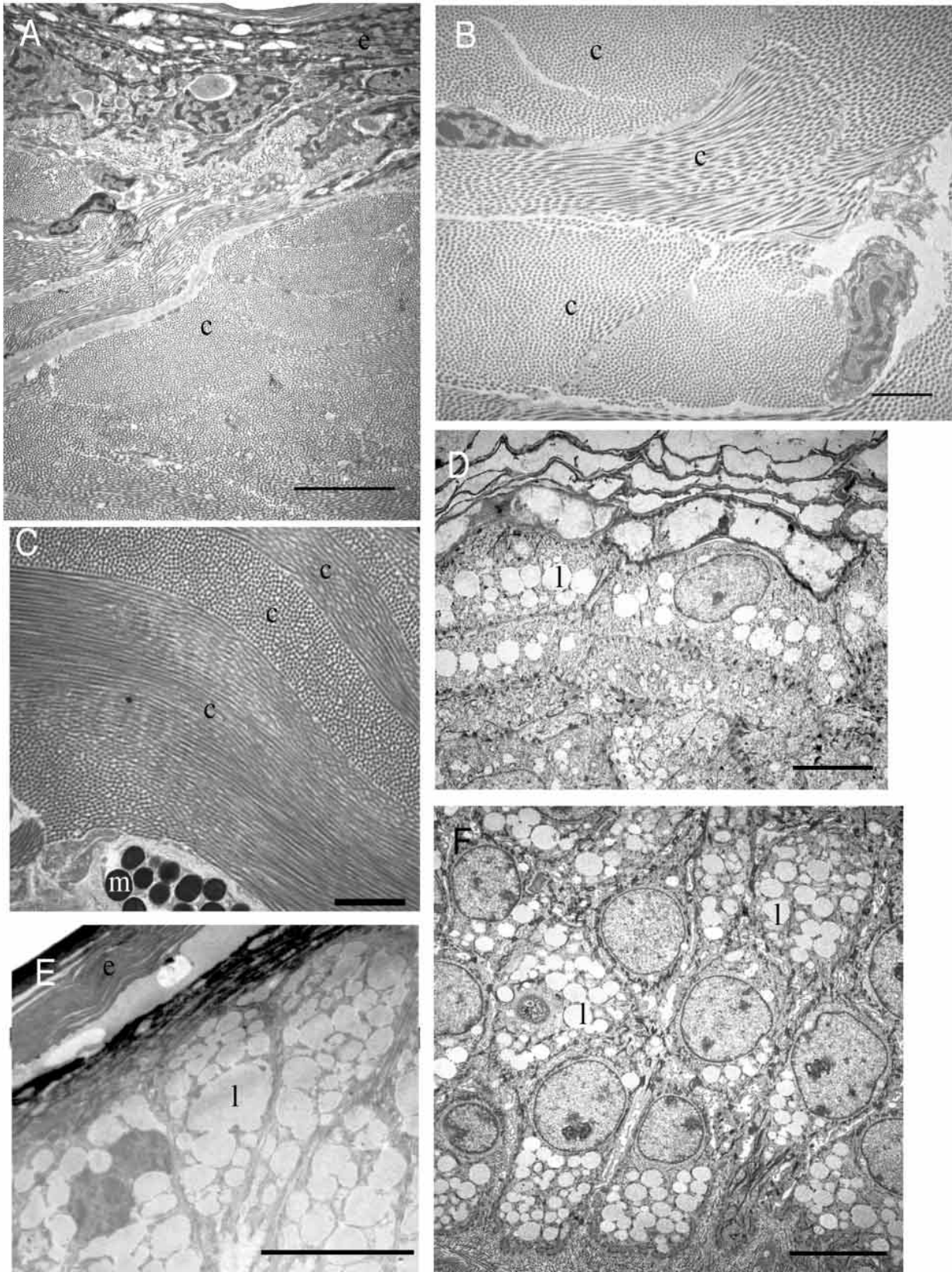


Fig. 6. Transmission electron micrographs of structurally coloured and carotenoid pigmented bird skin. Collagen macrofibrils of (A,B) *Tragopan satyra* and (C) *Tragopan caboti*. Lipid-filled pigment cells immediately under the epidermis in (D) *Dyaphorophyia concreta* yellowish green, (E) *Tragopan caboti* orange and (F) *Ramphastos toco* yellow. Scale bars represent 5 μm (A,D–F) or 2 μm (B,C). Abbreviations: c, collagen macrofibrils; e, epidermis; l, lipid vacuoles; m, melanosomes.

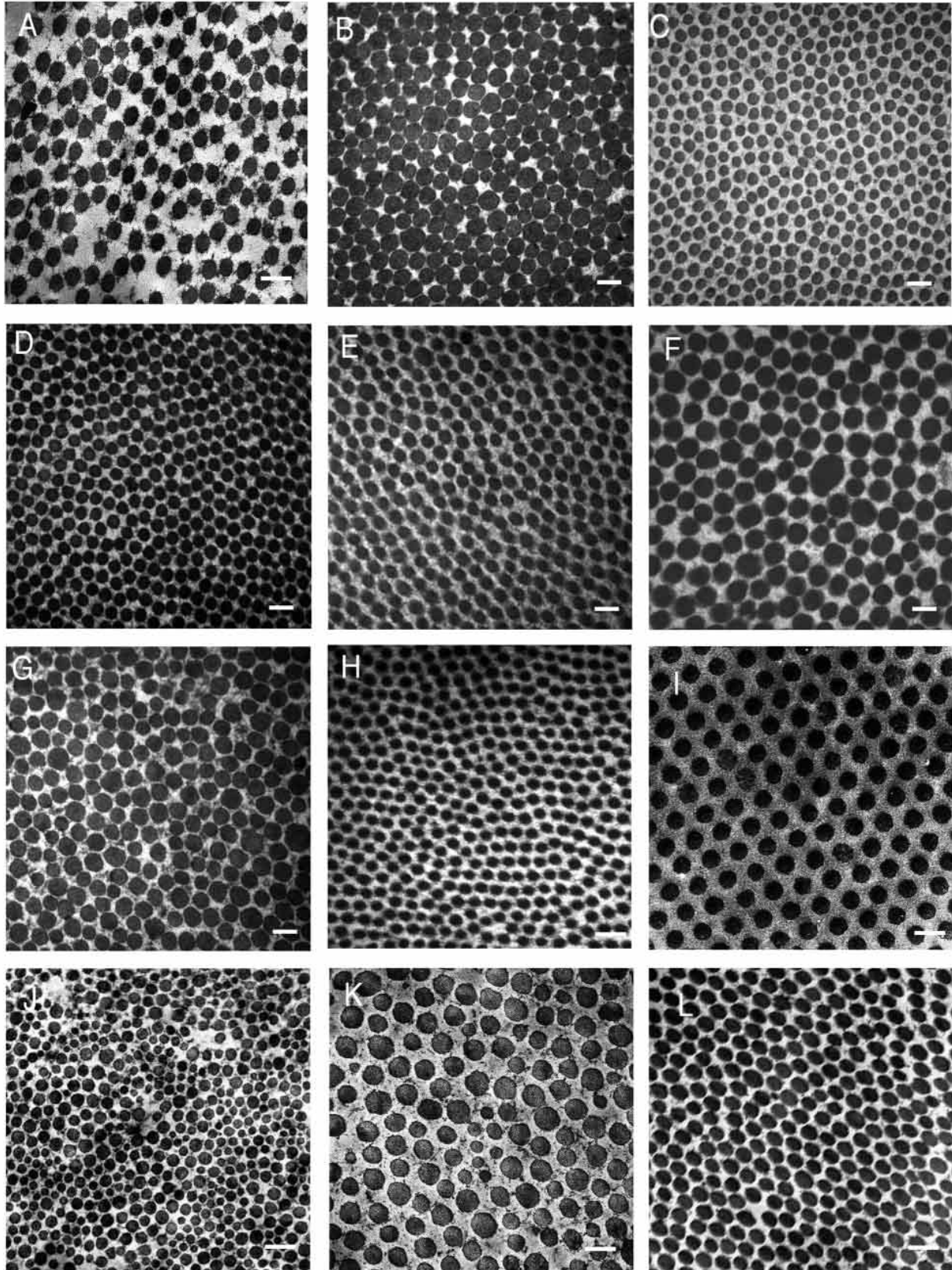


Fig. 7. Transmission electron micrographs of nanostructured arrays of dermal collagen from: (A) *Oxyura jamaicensis*, light blue; (B) *Numida meleagris*, dark blue; (C) *Tragopan satyra*, dark blue; (D) *Tragopan caboti*, dark blue; (E) *Tragopan caboti*, light blue; (F) *Tragopan caboti*, orange; (G) *Syrigma sibilatrix*, blue; (H) *Ramphastos toco*, dark blue; (I) *Philepitta castanea*, light blue; (J) *Gymnopithys leucapsis*, light blue; (K) *Procnias nudicollis*, green and (L) *Terpsiphone mutata*, dark blue. All images were taken at 30000 \times . All scale bars represent 200 nm.

vacuoles and has abundant underlying melanosomes. Some tissues, including the yellow facial skin of *R. toco*, apparently combine both structural colouration and carotenoid pigmentation (see ‘Combined structural and pigmentary colours’ below).

Nanostructure

Quasi-ordered arrays of parallel collagen fibres were observed in the dermis of 30 of the 31 species examined (Fig. 7). Collagen fibres were identified by their circular cross-sections and by the distinctive collagen banding pattern when viewed perpendicular to the fibre axes (Fig. 6A–C). In the quasi-ordered arrays, the collagen fibres were similar in diameter and interfibre distance but were not arranged in a crystal-like lattice or laminar organization (Fig. 7). Only one species, *P. castanea* (Fig. 7I), had collagen arrays organized in a highly regular, crystal-like, hexagonal nanostructure (Prum et al., 1994, 1999a).

The arrays of dermal collagen fibres were organized in

larger, lozenge-shaped structures, called macrofibrils by Prum et al. (1994, 1999a), which are apparently produced by a single collagenocyte during development (Fig. 6A–C). These collagen macrofibrils varied between 5 μm and 20 μm in diameter and were 20–100 μm long (Figs 5, 6A–C). The main axis of most of these collagen fibres runs roughly parallel to the surface of the skin, although there is substantial variation (Figs 5, 6A–C).

No specimens exhibited any evidence of iridophores – pigment cells that contain arrays of purine or pterine crystals and produce structural colours in the integument of fishes, amphibians and reptiles (Bagnara and Hadley, 1973; Fox, 1976; Bagnara, 1998) and in the avian iris (Ferris and Bagnara, 1972; Oliphant et al., 1992; Bagnara, 1998). Most samples showed no epidermal lipid vacuoles that may contain carotenoid pigments (Lucas and Stettenheim, 1972; Menon and Menon, 2000), but combined structural and pigmentary colours in *T. caboti*, *Apaloderma aequatoriale*, *R. toco* and *D. concreta* are discussed below.

2-D Fourier analysis

Two-dimensional Fourier analysis was used to describe the spatial periodicity of the variation in refractive index within the colour-producing dermal collagen arrays. The 2-D Fourier power spectra of TEM images of cross-sections of the collagen arrays exhibit circular rings of high magnitude power values at intermediate spatial frequencies (Fig. 8). Some power spectra reveal a second high power ring of harmonic spatial frequencies at twice the magnitude of the fundamental spatial frequency (Fig. 8A,B,D,F,H,I). Radial means of these power spectra indicate that these peak spatial frequencies vary between 0.0049 nm^{-1} and 0.0097 nm^{-1} among the differently coloured skin samples from different species (Fig. 9; Table 2; but see ‘Structural colour production in antbird skin’ below). This range of spatial frequencies corresponds to centre-to-centre distances between neighbouring collagen fibres of 110–204 nm (Prum et al., 1999a). This range of spatial frequency values should result in coherently scattered colours within the visible spectrum of birds (Fig. 9).

The ring-shaped Fourier power distributions of most species demonstrate that these collagen arrays are substantially nanostructured

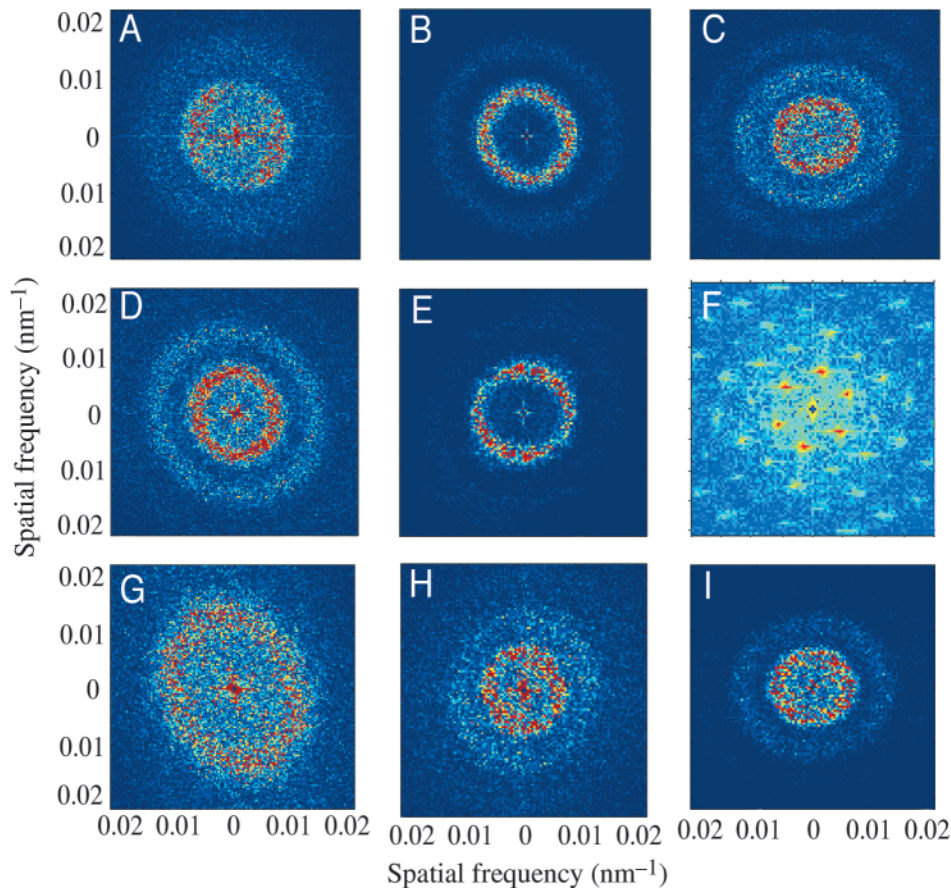


Fig. 8. Two-dimensional Fourier power spectra of transmission electron micrographs of nanostructured collagen arrays from: (A) *Dromaius novaehollandiae*, blue; (B) *Tragopan satyra*, dark blue; (C) *Ptilerodius pileatus*, light blue; (D) *Coua reynaudii*, dark blue; (E) *Ramphastos toco*, dark blue; (F) *Philepitta castanea*, light blue; (G) *Gymnophithys leucapsis*, light blue; (H) *Procnias nudicollis*, green and (I) *Dyaphorophyia concreta*, yellow green. Colours (from blue to red) indicate the magnitude of the squared Fourier components, which are in dimensionless units. Ring diameter is inversely proportional to the peak wavelength of the coherently scattered colour.

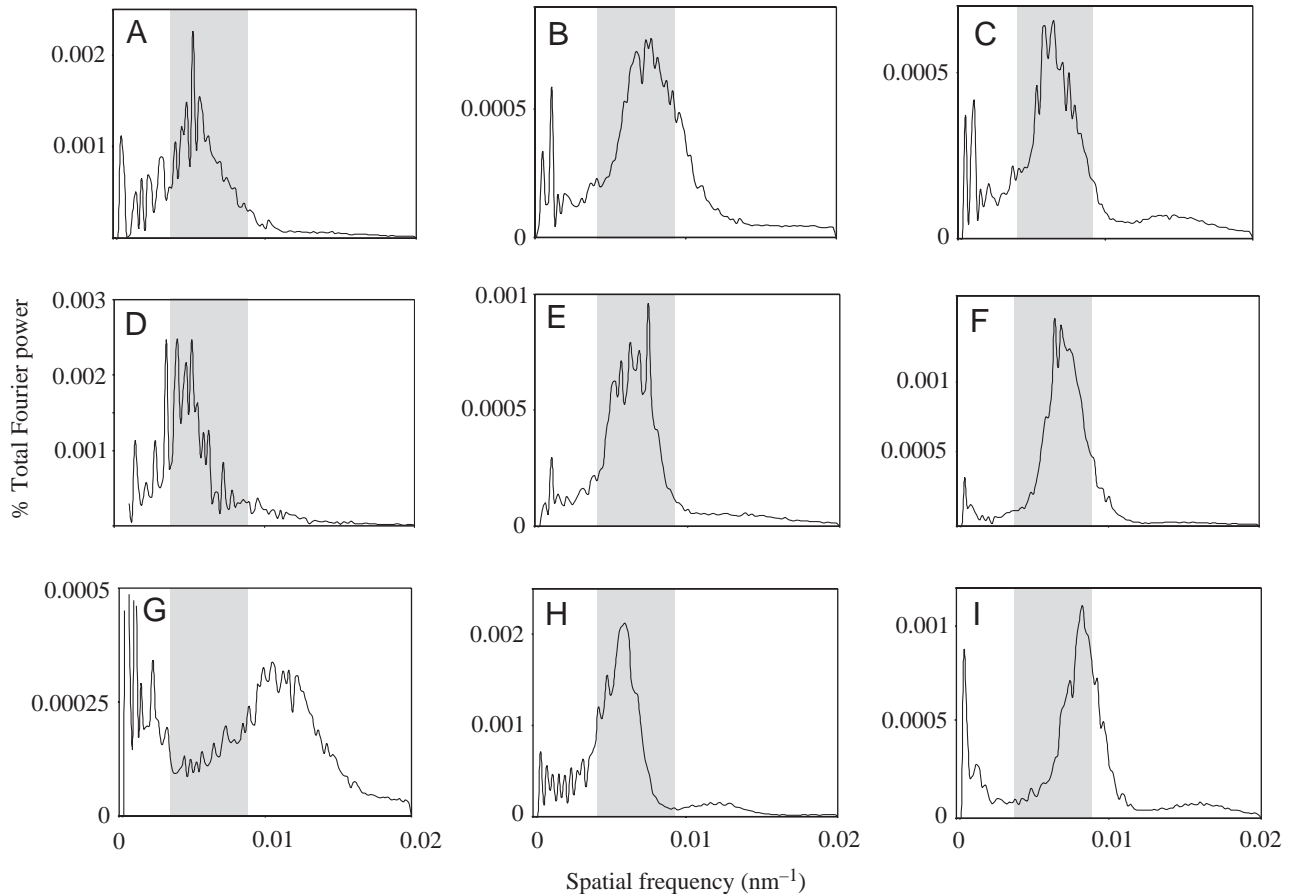


Fig. 9. Radial means of the two-dimensional Fourier power spectra of transmission electron micrographs of avian dermal collagen arrays: (A) *Oxyura jamaicensis*, light blue; (B) *Tragopan temminckii*, dark blue; (C) *Tragopan temminckii*, light blue; (D) *Tragopan caboti*, orange; (E) *Coua reynaudii*, dark blue; (F) *Ramphastos toco*, dark blue; (G) *G. leucapsis*, light blue; (H) *Dyaphorophya concreta*, green and (I) *Terpsiphone mutata*, dark blue. The shaded zones show the range of spatial frequencies that are likely to produce coherent scattering of visible light wavelengths. *G. leucapsis* has a larger peak spatial frequency that falls outside the range of values likely to produce a visible colour by coherent scattering.

(Fig. 8). Furthermore, the predominant nanostructure is of the appropriate size to produce visible hues by coherent scattering (Fig. 9). The circular rings in the power spectra further demonstrate that the dermal collagen fibre arrays are quasi-ordered or equivalently nanostructured in all directions perpendicular to the fibres. The circular power spectra demonstrate that these collagen arrays lack the laminar or crystal-like periodicity found in highly iridescent, coherently scattering nanostructures. Thus, congruent with their appearance, ring-shaped 2-D Fourier spectra predict that the collagen arrays should not be strongly iridescent. There is also substantial variation in orientation of collagen arrays both in angle to the epidermis and in fibre orientation at larger spatial scales (Figs 5, 6A–C), which further eliminates opportunities for iridescence at larger spatial scales. The unique, hexagonal arrays of *P. castanea* (Fig. 7I) produced power spectra with a hexagonal distribution of high power values (Fig. 8F; Prum et al., 1999a). However, *P. castanea* is also not iridescent because the many collagen arrays in the dermis are arranged in many different angles and directions with respect to the skin,

eliminating the hexagonal order of the nanostructure (Prum et al., 1999a).

The demonstration of substantial nanostructure at these spatial scales ($0.0049\text{--}0.0097\text{ nm}^{-1}$) directly falsifies a fundamental assumption of the incoherent scattering mechanisms, including Rayleigh (Tyndall) and Mie scattering (Figs 8, 9). The light-scattering collagen fibres in these tissues are not spatially independent (i.e. randomly distributed at the spatial scale of visible wavelengths) as the incoherent scattering models assume.

Predicted reflectance spectra based on the 2-D Fourier power spectra correspond generally to the observed colours of the original tissues (Fig. 10; Table 2). Accurate quantitative predictions of the peak wavelengths (λ_{max}) of the reflectance spectra of these tissue samples were limited by the variable condition of the original specimens (e.g. frozen or fresh), by variable collection circumstances, by different original fixatives (10% formalin vs glutaraldehyde) and especially by degradation of nanostructure and refractive index between the time of fixation and TEM examination (see ‘Sources of error’

below). The 2-D Fourier method, however, did provide accurate predictions of tissue colours for those specimens that were fixed and examined with TEM in a relatively short time period (less than six months; Fig. 10). For example, the predicted reflectance spectra match the measured reflectance spectra well for *T. temminckii*, *T. caboti*, *L. bulweri*, *Pilherodius pileatus*, *Syrigma sibilatrix*, *Selenidera culik*, *R. toco* and *D. concreta*. In particular, the variation in colour between dark blue and light blue portions of the caruncle shield of *T. temminckii* and *T. caboti* was accurately predicted by the Fourier analysis of the nanostructures of the collagen arrays from these parts of the tissues (Fig. 10B–D; Table 2). Thus, the Fourier analyses further support the conclusion that the hue of coherent scattering is determined by mean collagen fibre size and interfibre spacing.

Coherent scattering from dermal arrays produces a wide variety of structural hues in bird skin from ultraviolet to yellow. Although it has been hypothesized that integumentary green colours are produced by structural blue with carotenoid yellows, the green colours in the skin of *S. culik*, *Selenidera reinwardtii*, *P. castanea*, *P. nudicollis* and *D. concreta* and the yellow colour of the skin of *Ceuthmochares aereus* are purely structural. These tissues lacked any indication of carotenoid-containing lipid vacuoles in the integument, and Fourier analysis of their collagen arrays indicates that the fibres are appropriately nanostructured to create the observed hues by coherent scattering alone.

Combined structural and pigmentary colours

Several species examined had areas of yellow and orange skin that appear to be produced by a combination of structural colouration and carotenoid pigmentation: the orange facial and lappet skin of the pheasant *T. caboti* (Fig. 2F), the yellow facial skin of the trogon *A. aequatoriale*, the yellow facial skin of *R. toco* and the yellowish portions of the circumorbital caruncle of the Old World flycatcher *D. concreta* (Fig. 3J). All four of these samples showed substantial concentrations of lipid-filled cells in the uppermost strata of the dermis (Fig. 6D,E). Pigments within these lipid vacuoles were not extracted or identified but are presumed to be carotenoids.

T. caboti, *R. toco* and *D. concreta* had other purely structurally coloured areas of dark blue, light blue or green skin that completely lacked lipid-filled pigment cells that were immediately adjacent to the carotenoid pigmented areas. In all three species, the collagen arrays in these adjacent structurally coloured areas were appropriately nanostructured to produce the observed colours entirely by coherent scattering alone (Table 2). The dermis of the orange skin of *T. caboti* is thick with collagen arrays and the underlying dermis is highly melanized, indicating that this orange hue is not produced by capillary blood as in the paired, lateral, red patches of the facial lappet of all *Tragopan* species (Fig. 2E,F). Critically, in the yellow and orange areas of *T. caboti*, *R. toco*, *A. aequatoriale* and *D. concreta* tissue, the collagen arrays showed substantially larger collagen fibre diameters (Fig. 7F,K) and smaller peak spatial frequencies ($0.0036\text{--}0.0061\text{ nm}^{-1}$; Figs 8I, 9D,H; Table 2), which should

coherently scatter longer-wavelength colours (Fig. 10D,I; Table 2). Thus, it appears that in some avian taxa, longer-wavelength yellow and orange integumentary colours are produced by a combination of longer-wavelength structural colour and carotenoid pigmentation.

The importance of the structural component to the colours of the orange *T. caboti* (Fig. 2F; Table 2) and the yellow *A. aequatoriale* (Table 2) skins is further supported by the shapes of their reflectance spectra (Fig. 4F). Typically, carotenoid pigments produce a long wavelength plateau in their reflectance spectra. By contrast, the orange and yellow skins of *T. caboti* (Fig. 4F) and *A. aequatoriale* (data not shown) reveal a distinct reflectance peak at 600 nm and 530 nm, respectively, with a substantial drop off in reflectance at longer wavelengths beyond the peak. Furthermore, the reflectance peaks are generally congruent with the predicted reflectance spectra based on the Fourier analysis of the collagen arrays in this tissue (Fig. 10D; Table 2). Since carotenoid pigments typically do not fluoresce (i.e. they cannot emit wavelengths different from excitation wavelengths), reduction in the backscattering of longer wavelengths into the carotenoid pigment cells would reduce the emission of longer wavelengths by those pigments. Apparently, destructive interference of longer wavelengths by the quasi-ordered dermal collagen arrays limits backscattering of longer wavelength light from the dermis into the more superficial carotenoid pigment cells. This selective coherent scattering of mid-range wavelengths by dermal collagen evidently reduces the typical long wavelength reflectance of the carotenoid pigments and produces a colour whose brilliance is probably enhanced by the presence of the pigments but which has a reflectance spectrum that is distinctly more saturated at intermediate wavelengths than those of typical pigmentary colours. By contrast, the yellow skin of *R. toco* has a reflectance spectrum with a broad plateau in reflectance across all longer wavelengths (550–750 nm; Table 2), which is typical of carotenoid pigments.

Structural colour production in antbird skin

The structurally coloured skin of one species of antbird (Thamnophilidae) examined, *Myrmeciza ferruginea*, was typical in collagen nanostructure and dermal melanization of the other bird species examined. However, two of the three species examined from the Neotropical suboscine antbirds, *G. leucapsis* and *R. melanosticta* (Thamnophilidae), had conspicuously smaller nanostructures than all other species examined. Peak spatial frequencies in these tissues – 0.0105 nm^{-1} and 0.0136 nm^{-1} , respectively – correspond to fibre-to-fibre centre distances of 67–74 nm. The circumorbital tissues of *G. leucapsis* and *R. melanosticta* are light blue in life (Fig. 3G), but, unlike all other samples, these tissues immediately lost their blue colour upon fixation and became nearly transparent. Furthermore, both species lack any dermal melanin. Dermal tissues of both species had prominent collagen fibre arrays, but the fibre sizes were extremely small (Fig. 7J) and the spatial frequency rings were very large (0.0105 nm^{-1} and 0.0136 nm^{-1} , respectively; Fig. 8G). These

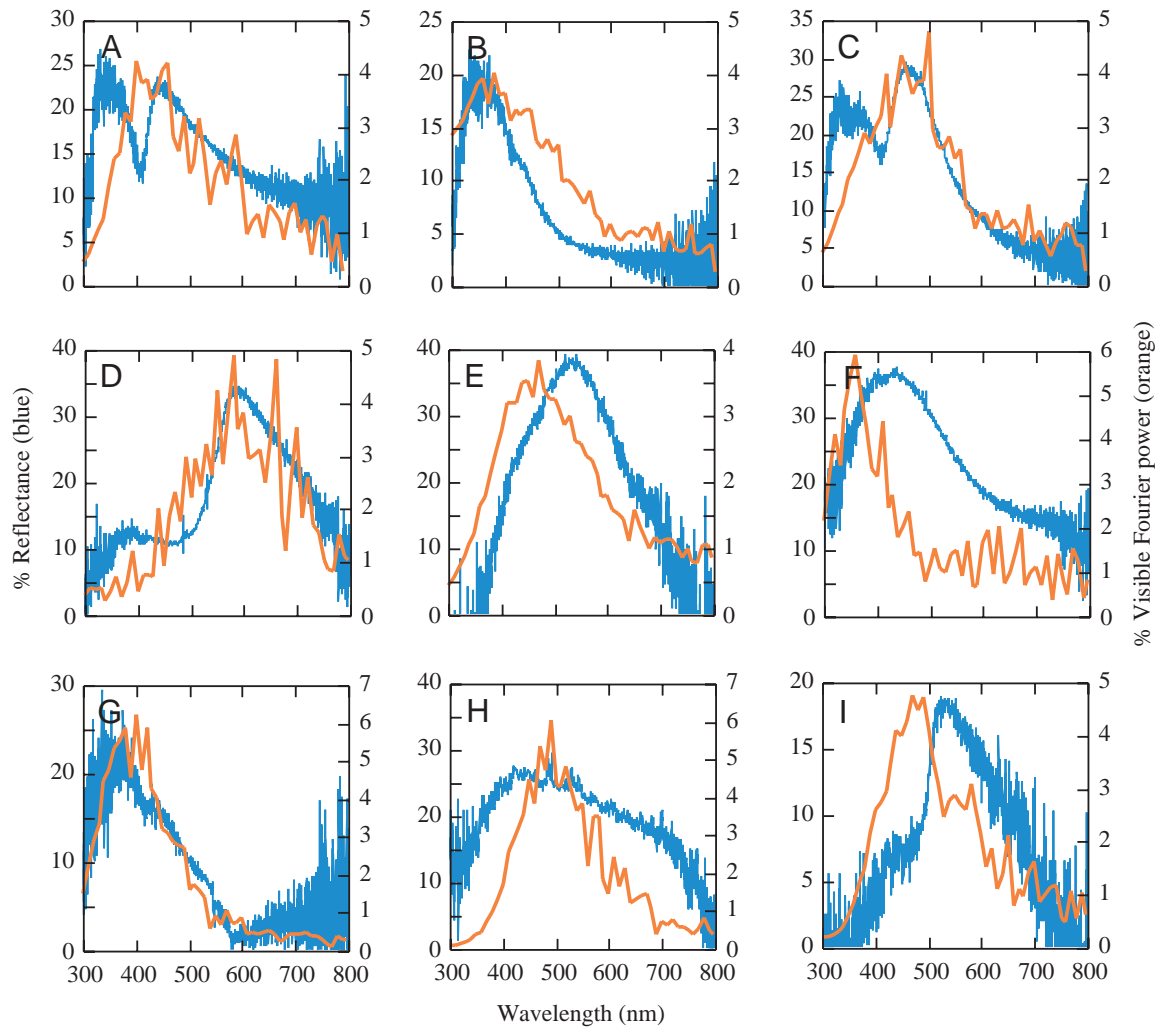


Fig. 10. Comparisons of measured reflectance spectra (blue) and Fourier-predicted reflectance spectra (orange) for a sample of structurally coloured avian specimens: (A) *Lophophorus impejanus*, dark blue; (B) *Tragopan temminckii*, dark blue; (C) *Tragopan temminckii*, light blue; (D) *Tragopan caboti*, orange; (E) *Syrigma sibilatrix*, light blue; (F) *Coua caerulea*, dark blue; (G) *Ramphastos toco*, dark blue; (H) *Selenidera culik*, green and (I) *Dyaphorophya concreta*, yellow-green. Reflectance spectra are reported as % reflectance (blue, left axis), and predicted reflectance spectra are reported as % visible Fourier power (orange, right axis).

fibre arrays are outside the range of sizes that are likely to make a visible colour by coherent scattering (Fig. 9G). Similar spatial frequencies in the collagen arrays of the human cornea create destructive interference among all visible wavelengths, producing optical transparency and coherent reinforcement of nonvisible light in the far ultraviolet (Benedek, 1971; Gisselberg et al., 1991; Vaezy and Clark, 1991, 1993). If *G. leucapsis* and *R. melanosticta* produce colour by coherent scattering from this nanostructure, it should be an extreme ultraviolet hue rather than the observed light blue. But this cannot be determined in the absence of reflectance spectrum of living specimens of these antbirds. Given these substantial differences in anatomy and nanostructure from the other coherently scattering tissues, it would be best to conclude that the mechanism of integumentary structural colour production in *Gymnopithys* and *Rhegmatorhina* antbirds remains to be established and requires further investigation.

Sources of error

In acquiring this sample of structurally coloured skin from a diversity of avian species from so many different sources, it was impossible to control for variation in preservation methods and conditions. The diverse specimens examined here were acquired over a period of eight years. Unfortunately, the colours of many specimens changed or degraded substantially after the original fixation during storage in cacodylate buffer at 4°C but before electron microscopy. Often, colours decreased in intensity to a greyish hue. Others also increased in wavelength with time. For example, the sample of light blue ramphotheca from *Oxyura jamaicensis* (Anatidae) had a peak reflectance of 465 nm in 1998 when the specimens were first thawed several days after death and fixed (Fig. 4A), but in 2002 at the time of the TEM observation the peak reflectance had changed to 590 nm. For this reason, accurate reflectance measurements could not be made for all species (Table 2).

Furthermore, Fourier analysis of some tissues predicted reflectance peaks that were of substantially longer wavelengths than the original colours. In the case of *Oxyura*, however, the measured (590 nm) and predicted (580 nm) hues after years of storage were closely correlated (Table 2).

Apparently, the observed changes in hue are the result of changes in the size of the colour-producing collagen arrays. Prum et al. (1994) hypothesized that shrinkage due to dehydration in 10% formalin and ethanol turned the green caruncle tissue blue in *P. castanea*. Likewise, the increase in hue in *Oxyura* is apparently a result of expansion in collagen array size during storage in cacodylate buffer following fixation. Alternatively, any changes in difference in refractive indices between the fixed collagen fibres and the surrounding mucopolysaccharide matrix could result in degradation in the magnitude of reflectance. For example, several samples (e.g. *Sula neboxii* and *C. aereus*) showed highly nanostructured collagen under TEM that should have produced vivid structural colours, but these preserved tissues were only dull grey in colour. Depending on the actual direction of change in mean refractive index of the tissue, the degradation of refractive indices could also contribute to increases or decreases in peak wavelength of reflectance.

Evolution of structurally coloured avian skin

The existence of anatomically identical collagen nanostructures that function by the same physical mechanism in many distantly related avian clades is compelling evidence of extensive convergent evolution. Unfortunately, higher level avian taxonomy is poorly understood, and there is no consensus phylogeny of birds. Homology among the many instances of avian structurally coloured skin would only be possible if these diverse genera were closely related and basal within their clades. However, many of these avian genera are members of diverse families in which there are many species that lack structurally coloured skin (Table 1). Furthermore, there is no reason to hypothesize that genera with structurally coloured skin are basal members of their families, that families including many genera with structurally coloured skin are basal within their orders or that families and orders with structurally coloured skin are especially closely related to one another. Thus, the hypothesis of homology among many or most instances of structurally coloured skin in birds would require numerous evolutionary losses and would be wildly unparsimonious.

Based on what is known about avian phylogeny, there is not a single unambiguous instance of homology of structurally coloured skin between any two avian families (Table 1). The structural colours of the anhingas (Anhingidae) and the cormorants (Phalacrocoracidae) come closest, but it is unlikely that the structurally coloured species within these families are basal. There are a few examples of diverse radiations of genera and species within families that potentially share a single origin of structurally coloured skin. For example, the guans and curassows (Cracidae), the pheasants (Phasianidae), the guineafowl (Numididae), the herons (Ardeidae), the hornbills

(Bucerotidae), the toucans (Ramphastidae), the monarch flycatchers (Monarchidae) and the honeyeaters (Meliphagidae) are clades with many genera and species that may share homologous, structurally coloured skin. Several genera or clades of genera have radiated with homologous structurally coloured skin patches: e.g. *Philepitta* and *Neodrepanis* (Eurylaimidae) and *Dyaphorophya* (Platysteiridae). By contrast, other families have probably had multiple evolutionary independent origins of this trait within them. A phylogeny of cotingas (Cotingidae) indicates that the three species with structurally coloured skin – *Perissocephalus tricolor*, *Procnias nudicollis* and *Gymnoderus foetidus* – are each most closely related to other species and genera that lack structurally coloured skin (Prum et al., 2000). Likewise, the bird of paradise genera *Paradigalla*, *Cicinnurus* and *Epimachus* (Paradisaeidae) are not hypothesized to be most closely related within the family (Frith and Beehler, 1998). Structurally coloured skin has probably had multiple independent evolutionary origins within New World and Old World cuckoos (Cuculidae; R. B. Payne, personal communication). Lastly, there are numerous instances of single, phylogenetically isolated species or genera with structurally coloured skin: e.g. *Cariama* (Cariamidae), *Opisthocomus hoazin* (Opisthocomidae), *Picathartes oreas* (Picathartidae), *Lopoparadisea* (Cnemophilidae), *Cyphorhynchus phaeocephalus* (Troglodytidae) and *Leucopsar rothschildi* (Sturnidae) (Table 1).

A precise estimate of the number of evolutionary origins and losses of structurally coloured skin in Aves would require a well-resolved phylogeny with accurate relationships from the highest interordinal levels to interspecific and intergeneric levels within many families. Based on the distribution of this trait among and within families of birds (Table 1), however, it would be conservative to estimate 50–65 evolutionarily independent origins of structurally coloured skin within extant birds.

Several instances of evolutionary radiation in structural colouration document that the hue of these structural colours can evolve rather easily in likely response to sexual and social selection (see Discussion). The collagen arrays of the yellow facial skin of *C. aereus* document that there are no physical constraints limiting the size of collagen fibre arrays and the colours they can produce. Four species observed – *T. caboti*, *A. aequatoriale*, *R. toco* and *D. concreta* – have evolved a combination of yellow and orange structural colours and carotenoid pigments. All species belong to diverse clades that have purely structurally coloured skin. Thus, it is possible in these clades that these combined structural pigmentary colours evolved from plesiomorphic structural colours with the derived addition of carotenoids.

Discussion

An investigation of the colour, anatomy and nanostructure of structurally coloured skin, ramphotheca and podotheca from a broad diversity of birds documents that these colours are produced by coherent scattering (i.e. constructive interference)

of light from arrays of parallel collagen fibres in the dermis. Variation in hue is created by variations in collagen fibre size and spacing. Previously described only in the Malagasy asities (Eurylaimidae; Prum et al., 1994, 1999a), these integumentary, colour-producing collagen arrays have convergently evolved in dozens of lineages of birds. The collagen arrays in all but one species observed here were quasi-ordered; the hexagonally ordered collagen arrays of *Philepitta castanea* (Eurylaimidae; previously described by Prum et al., 1994, 1999a) are unique among known animals.

Two-dimensional Fourier analysis of these colour-producing collagen arrays demonstrates that they are substantially nanostructured at the appropriate spatial scale to produce visible colours by coherent scattering (i.e. constructive interference). This quasi-ordered nanostructure is equivalent in all directions in the tissue perpendicular to the collagen fibres, which explains why these colours are not iridescent. In well-preserved tissues that are examined quickly, the 2-D Fourier analysis can provide an accurate prediction of the shape of the reflectance spectrum. No differences were found in anatomy or nanostructure among the structurally coloured skin, ramphotheca (*Oxyura jamaicensis* and *Ramphastos vitellinus*) or podotheca (*Sula nebouxii*).

The reflectance spectra of structurally coloured bird skin falsify the inverse fourth power prediction of the incoherent (Rayleigh) scattering hypothesis (Fig. 4). Furthermore, the ring-shaped maxima of the Fourier power spectra demonstrate directly that spatial variations in refractive index within these extracellular matrices are not spatially independent, as assumed by the incoherent scattering hypothesis (Figs 8, 9). After more than one century of unquestioned support, the Rayleigh (also known as Tyndall) scattering hypothesis has been falsified for a wide diversity of birds.

These results further discredit the common opinion among biologists that coherent scattering, or interference, is synonymous with iridescence (Mason, 1923; Fox, 1976; Nassau, 1983; Lee, 1991, 1997; Herring, 1994). Actually, both iridescent and non-iridescent structural colours can be produced by coherent scattering. Lamellar and crystal-like arrays can produce iridescence. Quasi-ordered arrays, however, are sufficiently nanostructured to produce vivid structural colours but are not appropriately ordered at larger spatial scales to create strong iridescence (Prum et al., 1998, 1999a,b). A simple review of previous citations of the Rayleigh scattering mechanism in biological systems indicates that this mechanism has never been satisfactorily demonstrated with the reflectance spectra that conform to the Rayleigh's predicted inverse fourth power law or with evidence of the spatial independence of light-scattering objects (Mason, 1923; Fox, 1976; Nassau, 1983; Herring, 1994; Parker, 1999). Given the historic lack of understanding of coherent scattering by quasi-ordered arrays, experimental re-evaluation of all proposed biological examples of Rayleigh scattering is required.

Our results demonstrate that nanostructured collagen in the avian dermis can be combined with carotenoid pigments to produce vivid integumentary colours. Furthermore, in some

species, coherent scattering of yellow and orange wavelengths by nanostructured dermal collagen results in a brilliant, pigment-enhanced hue that is more saturated than typically carotenoid pigment colours. Exploiting a similar phenomenon, artists often coat canvases with a preliminary layer of brilliantly white gesso to enhance the colour of their pigments. In some birds, however, a specific, underlying, coherently scattered hue serves to actually alter the colour of the superficial pigments by limiting long wavelength scattering. In the future, the presence of carotenoid pigments in the skin should not be sufficient to conclude that an integumentary colour is purely pigmentary, because there remains the possibility that carotenoid hues may be enhanced or altered by an underlying structural component. Specifically, the presence of integumentary carotenoid pigmentation with a discrete peak in the reflectance spectrum may indicate a structural component. This phenomenon should be looked for in birds, other reptiles, amphibians and fishes.

Two of the three genera of Neotropical antbirds (Thamnophilidae) provide the only exception among the structurally coloured bird skins examined. The dermal collagen arrays in these genera are so small that they should be optically transparent or should produce an extremely ultraviolet colour rather than the observed light blue hues. Additional investigation with better specimens and reflectance spectra from life are required to further investigate the mechanism of colour production in these genera. Furthermore, the double peaks in some galliform reflectance spectra (Fig. 4A–C,E) were not predicted by the Fourier analysis of the collagen nanostructure and may indicate the existence of some selective absorption of light at approximately 400 nm in the epidermis of these species.

Primitively, fishes, amphibians and reptiles produce integumentary structural colours with iridophores, specialized pigment cells in the dermis that contain guanine or pterine crystals (Bagnara and Hadley, 1973; Bagnara, 1998), but iridophores are absent from structurally coloured bird skin. These results confirm the conclusion that birds, like mammals, have evolutionarily lost integumentary iridophores (Oliphant et al., 1992; Bagnara, 1998), although birds retain iridophores as an important mechanism of structural colour production in the iris (Oehme, 1969; Ferris and Bagnara, 1972; Oliphant, 1981, 1987a,b; Oliphant et al., 1992; Oliphant and Hudon, 1993).

In at least two lineages – *Oxyura* (Anatidae) and the Malagasy asities (Eurylaimidae) (Figs 2B, 3D,E) – structurally coloured integumentary ornaments are seasonally variable. In *Oxyura*, males develop blue ramphotheca colouration during the breeding season (April–July) but have black bills during the rest of the year (Hays and Habermann, 1969). In asities, the structurally coloured facial caruncles develop in the breeding season and atrophy completely (including the dermal melanosomes and muscles) during the rest of the year (Prum and Razafindratsita, 1997; Prum et al., 1999a). All other structural colours in avian skin are apparently permanent once developed. One bird not examined here shows change in the

colour of the facial caruncle during ontogeny. In the blue-faced honeyeater *Entomyzon cyanotis* (Meliphagidae), adults have blue facial skin but immature individuals have greenish facial skin. Apparently, the ontogeny of colour in *Entomyzon* is characterized by a reduction in collagen nanostructure, which creates a shift in hue. The head and neck of wild turkey *Meleagris gallipavo* can change rapidly from white to blue (Schorger, 1966; A. Krakauer, personal communication). This rapid colour change may occur by mobilization of melanosomes within melanocytes in the dermis in response to hormonal cues, as in amphibians and other reptiles (Bagnara and Hadley, 1973; Bagnara, 1998), but this hypothesis has not been examined.

The 2-D Fourier method provides a new tool for the analysis of nanostructure and optical function in biological tissues (Prum et al., 1998, 1999a,b). The method is effective in testing alternative physical hypotheses of structural colour production. Under the best conditions that limit shrinkage or degradation of extracellular matrix nanostructure, the method provides an accurate prediction of the reflectance spectra of structurally coloured skin. Future research may be able to use the method to analyze the nanostructural basis of behaviourally relevant variation in structurally coloured hues within populations and species.

Evolution of avian structurally coloured skin

Two fundamental evolutionary questions are: how have these structurally coloured collagen arrays evolved and why has convergent evolution of these arrays been so frequent? Collagen is a ubiquitous and abundant extracellular matrix molecule in connective tissues of metazoan animals. Despite its diversity in molecular sequence, all collagens form self-assembled, triple-helical fibres that are composed of collagen polypeptides and are surrounded by a mucopolysaccharide matrix. Structural colour production by arrays of collagen fibres requires the appropriate specification of two components of collagen nanostructure that are already intrinsic to collagen itself – fibre diameter and interfibre spacing. Furthermore, the functional contribution of collagen to the elasticity and support of the integument ensures that a substantial component of dermal collagen fibres will be arranged parallel to the surface of the skin (D. Homberger, personal communication).

Thus, the collagenous extracellular matrix of the skin provides an inherent nanostructure that is very near to the appropriate spatial frequency and orientation to produce visible hues. Selection of integumentary collagen for a colour production function requires more rigid specification of pre-existing features of this extracellular matrix. Latent genetic variation in the nanostructure of integumentary collagen may occasionally create heritable, visible variations in reflectance that could become subject to subsequent natural, sexual or social selection for structural colour production. We proposed that the frequent, convergent exaptation of integumentary collagen for a novel colour production function in birds has been fostered by the nature and function of integumentary collagen itself. Interestingly, the broad visual sensitivity of birds to near-ultraviolet light would permit them to observe

optical consequences of a broader class of latent variations in integumentary collagen nanostructure and may create a broader set of opportunities for the evolution of nanostructured, colour-producing collagen from plesiomorphic collagen in the skin.

At larger anatomical scales, the evolution of structural colour production by integumentary collagen also requires the development of a sufficient number of light-scattering arrays to produce an observable colour. The reflectance (R ; i.e. the proportion of ambient light scattered at a single interface between two materials of different refractive indices) is calculated by the Fresnel equation to be:

$$R = [(n_D - n_A)/(n_D + n_A)]^2, \quad (2)$$

where n_D and n_A are the refractive indices of the two materials (Huxley, 1968; Land, 1972; Hecht, 1987). For other structural colour-producing, composite biological media, R varies widely: 4.8% (chitin–air), 2.5% (guanine–water) and 4.5% (keratin–air) (Land, 1972). These high- R biological arrays can produce nearly total reflection of all ambient light with 10–20 layers of light-scattering objects (Land, 1972). However, the difference in refractive index between collagen ($n=1.42$) and the mucopolysaccharide ($n=1.35$) is much smaller, yielding an R of approximately 0.05%. Collagen arrays need two orders of magnitude more scattering opportunities to produce the same magnitude of reflectance as these other colour-producing arrays. Thus, the evolution of structurally coloured skin in birds has required the proliferation of nanostructured dermal collagen arrays to produce a thicker dermis than in normal skin. Based on the thickness of the colour-producing dermal layer and the distance between adjacent fibres, the avian tissues examined typically include 500–2000 light-scattering collagen fibres in any dermal cross-section. Exceptionally, the colour-producing dermis of *Procnias nudicollis* (Cotingidae) includes more than 5000 fibres in a single cross-section (Figs 3H, 5H; see below).

The evolution of integumentary structural colouration also requires the development of a physical mechanism to prevent incoherent scattering of white light by deeper tissues that underlie the superficial colour-producing nanostructures. In almost all the species examined, colour-producing collagen arrays are underlain by a thick layer of melanin granules (Fig. 5). The anatomical association between integumentary structural colouration and melanin deposition is so strong that the melanin granules were frequently hypothesized to produce the colour themselves by Rayleigh scattering (Mandoul, 1903; Rawles, 1960; Hays and Habermann, 1969; Fox, 1976). Several authors have remarked that the disappearance of the structural colour upon removal of the melanin layer supports the conclusion that melanin actually produces the colour (e.g. Hays and Habermann, 1969). Actually, the functional role of underlying melanin is to absorb any light transmitted completely through the array and to prevent incoherent scattering of white light from the deeper tissues, which are not nanostructured for colour production. A functional alternative to an underlying melanin barrier is to have enough light-scattering objects in the array so that virtually all the incident

light is coherently scattered in the appropriate hue. Thus, the approximately 5000 light-scattering collagen fibres in a dermal cross-section in *P. nudicollis*, which lacks dermal melanin (Fig. 5H), approaches the theoretical level of total reflection of incident light that would render any underlying melanin layer unnecessary.

Pre-existing melanin deposition in the skin may enhance the likelihood of subsequent evolution of structural colouration within a lineage by making the optical effects of chance variation in superficial collagen nanostructure immediately more visible. Many bird genera with structurally coloured skin have close relatives with melanin-pigmented facial skin: e.g. cormorants (Phalacrocoracidae), ducks (Anatidae), avocets (Recurvirostridae) and honeyeaters (Meliphagidae). Likewise, plesiomorphic bare skin may also foster the evolution of structurally coloured skin, since variations in integumentary nanostructure would be immediately observable and potentially subject to selection. The featherless eye ring is a good example of a broadly distributed bare skin, and, not surprisingly, the most common position for structural colours is around the eyes (Figs 2, 3).

There is at least one instance of evolution of integumentary structural colour by artificial selection in a domestic breed of chicken (*Gallus gallus*). Silkie chickens were first bred in China more than a thousand years ago. Silkies have many associated novel phenotypic features that evolved by artificial selection during domestication. These include feather abnormalities, polydactyly, highly melanized skin, albino feathers and deep blue to turquoise earlobes. It is likely that the original mutation in Silkie that produced extreme dermal melanization, unique in *Gallus*, created the opportunity for subsequent artificial selection for structurally coloured blue earlobes.

Function of integumentary structural colours

Little is known about the function of structural coloured skin in the lives of birds. Structurally coloured ornaments feature prominently in the courtship displays of some polygynous species. During the courtship displays of the polygynous male tragopans (*Tragopan*; Phasianidae), the throat lappet is extended over the breast by the shunting of blood, exposing complex patches of structural ultraviolet, structural light blue and pigmentary blood red hues; simultaneously, a pair of structurally coloured light blue horns is erected from the sides of the crown by the contraction of helical or cylindrically arranged muscles fibres (Murie, 1872; R. O. Prum, personal observation). The elongate, ultraviolet coloured facial caruncles of Bulwer's pheasant *Lophura bulweri* (Phasianidae) are erected by a combination of vascular and muscular mechanisms during its courtship displays (Fig. 2D; Schneider, 1938). In the velvet asity *Philepitta castanea* (Eurylaimidae), the two structurally coloured green and blue supraorbital caruncles are erected by muscular contraction to form two brilliant planes that intersect above the bill like a V-shaped, tricorner hat (Prum and Razafindratsita, 1997). Thus, in some lineages (e.g. Phasianidae, Eurylaimidae, Cotingidae,

Paradisaeidae and Cnemophilidae), the evolution and radiation of sexually dimorphic skin structural colours is associated with polygyny and consequent sexual selection. However, there are as many instances of sexually monomorphic skin structural colours (Ardeidae, Cariamidae, Bucerotidae, Ramphastidae, Meliphagidae, Monarchidae, etc.). Apparently, in other instances, integumentary structural colours have evolved in both sexes for other social communication purposes.

Although birds with structurally coloured skin are phylogenetically and ecologically diverse, the trait appears to have evolved most frequently in interior humid rainforest birds. For example, nearly all species with structurally coloured skin within the Casuariiformes, Galliformes, Opisthocomiformes, Cuculiformes, Trogoniformes, Coraciiformes, Piciformes and Passeriformes are found in tropical forests and woodlands, mostly in lowland tropical forests. Since tropical forest species account for a large proportion of all birds, it is ultimately necessary to test phylogenetically whether the observed frequency of structurally coloured skin among tropical forest birds is higher than random. However, the striking and complete conformity to this pattern within Passeriformes, which is diverse in both tropical and temperate habitats, provides strong support for the pattern. Although not predicted by previous sensory drive theory (Endler, 1993), the quality of ambient light within tropical forest habitats may foster convergent evolution of communication signals in the smaller wavelength portion of the visible spectrum, in which vertebrate pigments are unavailable. Vorobyev and Osorio (1998) have hypothesized that receptor noise is an important determinant of colour perception thresholds. Their model of tetrachromatic bird vision predicts that ultraviolet and blue sensitivity should rise in habitats where ultraviolet and blue wavelengths are rare (Vorobyev and Osorio, 1998). Endler (1993) has shown that smaller visible wavelengths are under-represented in tropical forest interiors under sun. Thus, smaller wavelength structural colours may have evolved more frequently in tropical forest and woodland birds in response to natural or sexual selection for signals that exploit increased visual sensitivity to these wavelengths in the ambient light environment.

We would like to thank the many individuals and institutions who made this research possible by donating specimens: Bret Benz, Kim Bostwick, Roger Boyd, Robert Faucett, Steve Goodman, Errol Hooper, LaDonna Lickteig, Nate Rice, Mark Robbins, David Watson, Kristof Zyskowski, the San Diego Zoo, the Topeka Zoo, the University of Kansas Natural History Museum and the Field Museum of Natural History. Jon Andrews, Alan Krakauer, Dominique Homberger and Robert B. Payne kindly provided helpful observations. Electron microscopy was conducted by Tim Quinn and Bruce Cutler. Light microscope histology was done by Rosetta Barkely. Scott Williamson and Christopher Fallen programmed the Fourier analysis software (available from R. O. Prum). Bret Benz helped with managing images. Funding for this research was provided by the National Science

Foundation (DBI-0078376, DMS-0070514). We would like to thank the following people and organizations for permission to reproduce photographs: Kenneth Fink, VIREO, Nate Rice and Roger Boyd.

References

- Auber, L.** (1957). The distribution of structural colors and unusual pigments in the Class Aves. *Ibis* **99**, 463-476.
- Bagnara, J. T.** (1998). Comparative anatomy and physiology of pigment cells in nonmammalian tissues. In *The Pigmentary System – Physiology and Pathophysiology* (ed. J. J. Nordlund, R. E. Boissy, V. J. Hearing, R. A. King and J. P. Ortonne), pp. 9-40. Oxford: Oxford University Press.
- Bagnara, J. T. and Hadley, M. E.** (1973). *Chromatophores and Color Change*. New Jersey: Prentice Hall.
- Bellairs, R., Harkness, M. L. and Harkness, R. D.** (1975). The structure of the tapetum of the eye of the sheep. *Cell Tissue Res.* **157**, 73-91.
- Benedek, G. B.** (1971). Theory of transparency of the eye. *Appl. Optics* **10**, 459-473.
- Bohren, C. F. and Huffman, D. R.** (1983). *Absorption and Scattering of Light by Small Particles*. New York: John Wiley & Sons.
- Briggs, W. L. and Henson, V. E.** (1995). *The DFT*. Philadelphia: Society for Industrial and Applied Mathematics.
- Burkhardt, D.** (1989). UV vision: a bird's eye view of feathers. *J. Comp. Physiol. A* **164**, 787-796.
- Camichel, C. and Mandoul, H.** (1901). Des colorations bleue et verte de la peau des Vertébrés. *Compte Rendu Seances Acad. Sci.* **133**, 826-828.
- Derim-Oglu, E. N.** (1994). Small passerines can discriminate ultraviolet surface colours. *Vision Res.* **34**, 1535-1539.
- Endler, J. A.** (1993). The color of light in forests and its implications. *Ecol. Monogr.* **61**, 1-27.
- Ferris, W. and Bagnara, J. T.** (1972). Reflecting pigment cells in the dove iris. In *Pigmentation: Its Genesis and Biological Control* (ed. V. Riley), pp. 181-192. New York: Appleton-Century-Crofts.
- Finger, E.** (1995). Visible and UV coloration in birds: Mie scattering as the basis of color production in many bird feathers. *Naturwissenschaften* **82**, 570-573.
- Fox, D. L.** (1976). *Animal Biochromes and Structural Colors*. Berkeley: University of California Press.
- Frith, C. B. and Beehler, B. M.** (1998). *The Birds of Paradise*. Oxford: Oxford University Press.
- Ghiradella, H.** (1991). Light and colour on the wing: structural colours in butterflies and moths. *Appl. Optics* **30**, 3492-3500.
- Gisselberg, M., Clark, J. I., Vaezy, S. and Osgood, T.** (1991). A quantitative evaluation of Fourier components in transparent and opaque calf cornea. *Am. J. Anat.* **191**, 408-418.
- Hart, N. S.** (2001). The visual ecology of avian photoreceptors. *Prog. Ret. Eye Res.* **20**, 675-703.
- Hays, H. and Habermann, H.** (1969). Note on bill color of the ruddy duck, *Oxyura jamaicensis rubida*. *Auk* **86**, 765-766.
- Hecht, E.** (1987). *Optics*. Reading, MA: Addison-Wesley Publishing.
- Herring, P. J.** (1994). Reflective systems in aquatic animals. *Comp. Biochem. Physiol. A* **109**, 513-546.
- Huxley, A. F.** (1968). A theoretical treatment of the reflexion of light by multi-layer structures. *J. Exp. Biol.* **48**, 227-245.
- Jacobs, G. H.** (1992). Ultraviolet vision in vertebrates. *Am. Zool.* **32**, 544-554.
- Land, M. F.** (1972). The physics and biology of animal reflectors. *Prog. Biophys. Mol. Biol.* **24**, 77-106.
- Lee, D. W.** (1991). Ultrastructural basis and function of iridescent blue colour of fruits in *Elaeocarpus*. *Nature* **349**, 260-262.
- Lee, D. W.** (1997). Iridescent Blue Plants. *Am. Sci.* **85**, 56-63.
- Leonard, D. W. and Meek, K. M.** (1997). Refractive indices of the collagen fibrils and extrafibrillar material of the corneal stroma. *Biophys. J.* **72**, 1382-1387.
- Lucas, A. M. and Stettenheim, P. R.** (1972). *Avian Anatomy – Integument*. Washington, DC: U.S. Department of Agriculture.
- Mandoul, H.** (1903). Recherches sur les colorations tégumentaires. *Annal Sci Natur B. Zool.* **8 Ser.**, **18**, 225-463.
- Mason, C. W.** (1923). Structural colors of feathers. I. *J. Phys. Chem.* **27**, 201-251.
- MATLAB** (1992). *MATLAB Reference Guide*. Natick: The Mathworks, Inc.
- Maurice, D. M.** (1984). The cornea and sclera. In *The Eye* (ed. H. Davson), pp. 1-158. New York: Academic Press.
- Menon, G. K. and Menon, J.** (2000). Avian epidermal lipids: functional considerations and relationship to feathering. *Am. Zool.* **40**, 540-552.
- Murie, J.** (1872). Cranial appendages and wattles of the horned tragopan. *Proc. Zool. Soc. Lond.* **1872**, 730-736.
- Nassau, K.** (1983). *The Physics and Chemistry of Color*. New York: John Wiley & Sons.
- Neville, A. C.** (1975). *Biology of the Arthropod Cuticle*. New York: Springer-Verlag.
- Neville, A. C.** (1993). *Biology of Fibrous Composites*. Cambridge: Cambridge University Press.
- Oehme, H.** (1969). Vergleichende Untersuchungen über die Färbung der Vogeliris. *Biologische Zentralblatt* **88**, 3-35.
- Oliphant, L. W.** (1981). Crystalline pteridines in the stromal pigment cells of the iris of the great horned owl. *Cell Tissue Res.* **217**, 387-395.
- Oliphant, L. W.** (1987a). Observations on the pigmentation of the pigeon iris. *Pigment Cell Res.* **1**, 202-208.
- Oliphant, L. W.** (1987b). Pteridines and purines as major pigments of the avian iris. *Pigment Cell Res.* **1**, 129-131.
- Oliphant, L. W. and Hudon, J.** (1993). Pteridines as reflecting pigments and components of reflecting organelles in vertebrates. *Pigment Cell Res.* **6**, 205-208.
- Oliphant, L. W., Hudon, J. and Bagnara, J. T.** (1992). Pigment cell refugia in homeotherms – the unique evolutionary position of the iris. *Pigment Cell Res.* **5**, 367-371.
- Osorio, D. and Ham, A. D.** (2002). Spectral reflectance and directional properties of structural coloration in bird plumage. *J. Exp. Biol.* **205**, 2017-2027.
- Parker, A. R.** (1999). Invertebrate structural colours. In *Functional Morphology of the Invertebrate Skeleton* (ed. E. Savazzi), pp. 65-90. London: John Wiley & Sons.
- Prum, R. O., Morrison, R. L. and Ten Eyck, G. R.** (1994). Structural color production by constructive reflection from ordered collagen arrays in a bird (*Philepitta castanea*: Eurylaimidae). *J. Morphol.* **222**, 61-72.
- Prum, R. O. and Razafindratsita, V. R.** (1997). Lek behavior and natural history of the velvet asity *Philepitta castanea* (Eurylaimidae). *Wilson Bull.* **109**, 371-392.
- Prum, R. O., Rice, N. H., Mobley, J. A. and Dimmick, W. W.** (2000). A preliminary phylogenetic hypothesis for the cotingas (Cotingidae) based on mitochondrial DNA. *Auk* **117**, 236-241.
- Prum, R. O., Torres, R. H., Kovach, C., Williamson, S. and Goodman, S. M.** (1999a). Coherent light scattering by nanostructured collagen arrays in the caruncles of the Malagasy asities (Eurylaimidae: Aves). *J. Exp. Biol.* **202**, 3507-3522.
- Prum, R. O., Torres, R. H., Williamson, S. and Dyck, J.** (1998). Coherent light scattering by blue feather barb. *Nature* **396**, 28-29.
- Prum, R. O., Torres, R. H., Williamson, S. and Dyck, J.** (1999b). Two-dimensional Fourier analysis of the spongy medullary keratin of structurally coloured feather barb. *Proc. R. Soc. Lond. Ser. B. Biol. Sci.* **266**, 13-22.
- Rawles, M. E.** (1960). The integumentary system. In *Biology and Comparative Physiology of Birds*, vol. 1 (ed. A. J. Marshall), pp. 189-240. New York: Academic Press.
- Schneider, A.** (1938). Bau und erektion der hautlappen von *Lobiophasis bulweri* Sharpe. *J. Ornithol.* **86**, 5-8.
- Schorger, A. W.** (1966). *The Wild Turkey; Its History and Domestication*. Norman, OK: University of Oklahoma Press.
- Srinivasarao, M.** (1999). Nano-optics in the biological world: beetles, butterflies, birds, and moths. *Chem. Rev.* **99**, 1935-1961.
- Tièche, M.** (1906). Über benigne melanome ("Chromatophore") der Haut – "blaue Naevi". *Virch. Arch. Pathol. Anat. Physiol.* **186**, 216-229.
- Vaezy, S. and Clark, J. I.** (1991). A quantitative analysis of transparency in the human sclera and cornea using Fourier methods. *J. Microsc.* **163**, 85-94.
- Vaezy, S. and Clark, J. I.** (1993). Quantitative analysis of the microstructure of the human cornea and sclera using 2-D Fourier methods. *J. Microsc.* **175**, 93-99.
- van de Hulst, H. C.** (1981). *Light Scattering by Small Particles*. New York: Dover.
- Vorobyev, M. and Osorio, D.** (1998). Receptor noise as a determinant of colour thresholds. *Proc. R. Soc. Lond. Ser. B. Biol. Sci.* **265**, 351-358.
- Young, A. T.** (1982). Rayleigh Scattering. *Phys. Today* **35**, 42-48.